

AD-A191 611

FIBRE OPTIC SENSOR SYSTEMS FOR DAMAGE CONTROL PHASE I
(U) TIC DEFENCE SYSTEMS PLC BOSILDON (ENGLAND) MARINE
SYSTEMS DIV W E BURNAGE ET AL. AUG 87 48338
NO0014-87-C-2005

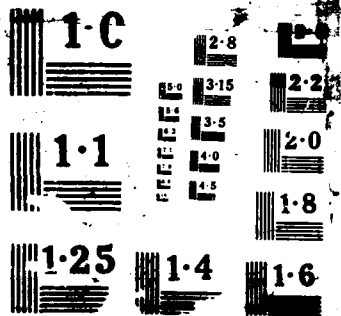
1/1

UNCLASSIFIED

F/G 14/2

ML

END
DATE
FILMED
8-



2

~~CONFIDENTIAL - CONFIDENTIAL~~

DTIC FILE COPY

REPORT 48330/1987

FIBRE OPTIC SENSOR SYSTEMS FOR DAMAGE CONTROL

Conceptual design of micromachined silicon fibre optic sensors for pressure, status and temperature monitoring and of a scatter cell based smoke detector.

Martin E. Burrage, J. Mark Naden, Richard J. Baker, Peter G. Hale, Simon E. Avis.

STC Defence Systems
Marine Systems Division
Chester Hall Lane
Basildon
Essex SS14 3BW
ENGLAND.

DTIC
ELECTE
JAN 12 1988
S D

AUGUST 1987

AD-A191 611

Final Phase One Report

Contract Number N00014-87-C-2085

DISTRIBUTION STATEMENT 1
Approved for public release;
Distribution Unlimited

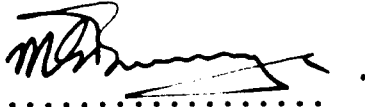
Prepared for

NAVAL RESEARCH LABORATORY
4555 Overlook Avenue, SW
Washington
DC 20375-5000

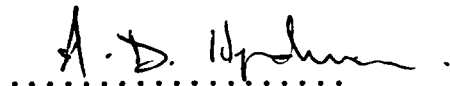
87 11 27 004

FIBRE OPTICS SENSOR SYSTEMS FOR DAMAGE CONTROL

Approvals



.....
DR. M. E. BURRAGE
Program Manager



.....
DR. A. D. HYNDMAN
MANAGER, ADVANCED PROJECTS.

Copyright Statement

Standard Telephones and Cables plc takes every precaution to ensure that the data and other material in this publication are correct and complete but as far as allowed by law will not accept liability for any death or personal injury, loss or damage arising from any error therein or omissions therefrom.

Standard Telephones and Cables plc does not warrant freedom from patent, copyright or other industrial property rights in respect of the use to which it may be put by the recipient.

No licence is granted by implication or otherwise under any patent, copyright or other industrial property right of Standard Telephones and Cables plc.

© 1987 Standard Telephones and Cables plc
Defence Systems Division, Basildon, ESSEX.

CONTENTS

Section		Page
1	INTRODUCTION	1
1.1	Project History	1
1.2	Conventional Sensors	1
1.3	Damage Control	3
1.3.1	Introduction	3
1.3.2	The nature of the risks	3
1.3.3	Damage Control Improvements	5
1.4	Fibre Optic Sensor Systems	5
1.4.1	Introduction	5
1.4.2	STC Fibre Optic Sensor Systems	6
2	OPTICAL SENSOR DESIGN	8
2.1	Introduction	8
2.2	The Common Optical Module	8
2.3	Transduction Methods	10
2.4	Multiplexing	13
3	SIGNAL PROCESSING	16
3.1	Introduction	16
3.2	Pre-processing	16
3.3	Demultiplexing	16
3.3.1	Digital methods	17
3.3.2	Analogue demultiplexing	18
3.4	Computer Interface	22
4	SMOKE DETECTORS	23
4.1	Introduction	23
4.2	Smoke Characteristics	23
4.3	Methods of Smoke Detection	24

Section	Page
4.4	24
4.5	26
4.6	26
5	28
5.1	28
5.2	28
5.3	29
6	30
FIGURES	35
REFERENCES	87
BIBLIOGRAPHY	90
APPENDIX A. Derivation of the resonant frequency of a silicon oscillator.	91
APPENDIX B. Calculation of the drive power for one sensor.	94
APPENDIX C. Temperature dependence of the Silicon oscillator.	95
Abbreviations, acronyms and symbols.	97

Accession For	
NTIS (GFA&I)	<input checked="" type="checkbox"/>
DTIC TAB	<input type="checkbox"/>
Unannounced	<input type="checkbox"/>
Justification	
By <i>per ltr</i>	
Distribution	
Availability Codes	
Dist	Availability for Special
<i>A-1</i>	

1. INTRODUCTION

1.1 Project History

The work described in this report was undertaken under NRL contract number N00014-87-C-2085 and was carried out between 14th April 1987 and 3rd August 1987. The work represents phase one, a conceptual design phase, of a four phase programme and is based on the STC response (Ref. 1) to an NRL request for proposal (RFP, Ref. 2).

The RFP sought the development of fibre optic sensor systems for damage control, system control or intrusion defence. STC's proposal addressed the development of frequency-out, microengineered fibre optic sensors for pressure, temperature and status monitoring and a fibre optic sensor, based on light scattering principles, for smoke detection. These sensors, and their associated signal processing, telemetry and display, formed the main elements of a system proposed for use in damage control.

The emphasis of the work under this programme has shifted somewhat from that originally proposed in order to reflect NRL's request for STC to focus on sensor capability, to limit effort on conventional system studies and to give a minimal treatment to aspects such as the use of MIL qualified components and the design of the telemetry and display parts of the system. The work has therefore tended to be application independent and is of relevance to other sensing applications in addition to those associated with damage control.

As was indicated in our original proposal, STC has developed a significant background capability in fibre optic sensors and, in particular, in microengineered silicon sensors. This private venture (p/v) funded work has continued since our proposal was made. The work has provided a useful basis for the present study and, in particular, the design of silicon paddle structures and their use in basic experimental sensors has been investigated. The results obtained have provided useful quantitative information which has been invaluable to the study made under this contract. Some of the results arising from p/v funded work have therefore been included in this report.

1.2 Conventional Sensors

Work on an examination of the limitations and operating problems associated with existing, conventional sensors used by the United States Navy (USN) has been limited at NRL's request. This was because NRL have conducted their own survey of these sensors and saw little need for further work in this area, particularly in view of our ability to produce a comprehensive survey within the limited context of this study. However, the NRL conclusions, as conveyed to us during the work, have been included here for completeness (Ref. 3).

NRL's work showed that there was no existing survey of the different sensors used on USN platforms. This situation has arisen because the number of sensor types, and the range of applications for which they are used, are so extensive that the preparation of a comprehensive, meaningful survey is difficult, if not impossible, to achieve. However, certain common problems and issues were identified.

Electromagnetic interference (EMI) is a general problem giving rise to degradation of the signal received from the sensor. This area is one where the introduction of fibre optic systems offers significant benefit. This advantage is generally recognised, together with other benefits of fibre optic systems, such as reduced cable weight and associated cost savings.

Sensor maintenance can be a problem, particularly for certain sensor types, e.g. level sensors. Specifically, float-type level sensors have been found to have a tendency for the float to stick and consequently for the sensor output to be false. Furthermore, these sensors can be difficult to remove for repair or replacement. The maintenance problem is essentially one of scale and of personnel requirements. A platform having a large number of sensors with a significant maintenance requirement necessitates the presence of dedicated, specialist personnel to carry out that function. There is an increasing need to minimise the numbers of such personnel required. A low maintenance requirement and, where necessary, maintenance which can be easily achieved are therefore key considerations in the development of any new sensor type.

A low occurrence of false alarms is also essential. A system which is unreliable in this way will tend to be ignored, or by-passed, by the users and will rapidly become of limited value. A system which can display faults and which can give a continuous read-out from its sensors, with alarm levels which can be programmed separately, is therefore to be preferred.

Smoke sensors are a particular sensor type where there is no satisfactory device currently available for use. Ionisation type smoke detectors have been removed from all USN platforms because of sensor unreliability and also because of concern about circumstances in which a large number of devices, each containing a small amount of radioactive material, are stored in close proximity. The development of a viable, new smoke detector is therefore of importance.

Greater than eighty per cent of the user requirement is represented by a limited range of sensors, viz. pressure, temperature, differential pressure and linear displacement sensors. There is therefore an understandable desire to emphasise the development of devices for making these measurements. In this context, the microengineered silicon sensors described in this report form a useful common basis from which transducers for different applications may be developed.

1.3 Damage Control

1.3.1 Introduction

Whilst the main thrust of the work reported here has been directed at the conceptual design of fibre optic sensors, it is appropriate to review briefly some aspects of the use of such sensor systems in damage control in a marine environment. The importance of the systems, and the context in which they may be used, will thereby be identified.

The extent of fire losses in the USN has been referred to in an NRL study which gives an analysis of the requirements for a consolidated damage control system (Ref. 4). Over a thirteen year period (1970-1982) there were 10,000 fires reported on ships and these resulted in a significant loss of life and cost. Over thirty of these fires cost over \$100K each and a few cost over ten million dollars each. It should be noted that none of these losses arose as a result of enemy action.

The importance of damage control provisions was given added impetus in the Royal Navy (RN) as a result of the Falklands war. Some of the lessons learned as a result of that conflict have been identified in a series of papers presented at a 1985 conference on Ship Fires (Ref. 5, 6 and 7). The incidence of fires on naval vessels in peace time, and also as a result of modern missile attack, is reviewed and the command and organisation structure and the nature of existing systems for damage control are described.

1.3.2 The nature of the risks

Existing methods of damage control have been noted as being inadequate in a number of respects and the following points summarise some of the problems encountered:

- (i) In the Falklands conflict, the detection, assessment and containment of fire proved difficult to achieve reliably and effectively (Ref. 7).
- (ii) In the absence of an adequate automatic detection system, there can be a considerable time lapse before the ships Damage Control Headquarters obtain an adequate picture of the damage. The lack of appropriate and reliable information on the ship and its installed systems (eg. the nature of flooding, status of compartments, availability of firemain) hampers the assessment and containment of damage (Ref. 7).

- (iii) An up-to-date and effective alternative Damage Control Headquarters has to be maintained. Damage control activities have been delayed when this has not occurred and when the main headquarters has had to be evacuated (Ref. 7).
- (iv) The arrangement and display of information, together with manual up-dating, does not provide easy assessment of damage effects. In the absence of decision making aids, the assessment is dependent on the Damage Control Officer's expertise and on his ability to analyse information displayed and to consider information transmitted from the incidents (Ref. 7).
- (v) In the case of the loss of the RN frigate HMS Sheffield, missile attack led to the loss of fire-fighting water together with the rapid spread of black smoke. The presence of smoke then prevented reconfiguration of the firemain (Ref. 5).
- (vi) Ventilation systems enable smoke and fire to spread through ships (Ref. 5).
- (vii) Automatic extinguishing systems are not always actuated effectively (Ref. 5).
- (viii) Fire is a more likely consequence of modern warfare than was the case in earlier conflicts (Ref. 5).
- (ix) Peacetime fires are more likely to occur in machinery spaces because of the presence of fuel, heat and heavy electrical machinery (Ref. 6). Clearly, in large vessels, having numerous unattended areas, the potential for fire developing in other spaces is much greater and constitutes a serious risk.
- (x) Missile explosion leads to a high temperature fire ball. Blast and fragments can damage fire-fighting systems, rupture fuel lines and ignite ammunition, adding to the severity of the fire. The ability to cut-off air supply and limit all openings in bulkheads is of critical importance in containing fires. Compressed air systems provide air to a fire if fractured and must be isolated. Breakage of fuel and hydraulic lines can also increase damage (Ref. 6).

- (xi) Fire and damage arising from missile attack represents one type of risk. Damage from other weapon types must also be considered and this can lead to structural failure with resultant flooding or fire or both. The extent to which the structure can be protected from the effects of modern weapons is limited. However, the ship design can be such that damage to the ship systems is controlled (Ref. 8).
- (xii) Damage control for fire and flooding is only one aspect of ship survivability. It must be considered in the wider context of nuclear - biological - chemical risks (Ref. 9 and 10).

1.3.3. Damage Control Improvements

A number of measures are being proposed and instituted to counter the risks highlighted above. These measures fall in the general areas of ship design, equipment, surveillance, organisation and training. In the case of the Royal Navy, the Type 23 frigate design has been modified to provide five, self-contained fire zones (Ref. 6 and 11) and current RN thinking on improvements to fire fighting equipment and its use is given in a number of papers (Ref. 5, 12 and 13).

The need for an integrated approach to damage surveillance and control is being recognised (Ref. 4 and 7). The development of sensors which are particularly suitable for use in such integrated systems will assist their development and eventual implementation. The work reported here can form part of such a development because the sensors which are envisaged will produce a digital output which would be compatible with advanced signal processing techniques.

1.4 Fibre Optic Sensor Systems

1.4.1 Introduction

A number of comprehensive reviews are available summarising the different approaches which may be adopted in the development of fibre optic sensors. A survey of these different techniques has not therefore been included in this report.

A review by NRL authors (Ref. 14) describes the development of fibre optic sensors for acoustic, magnetic and gyro applications in particular, together with the range of possible sensing techniques which have been examined for other applications.

A later review (Ref. 15) gives an assessment of the different techniques, with the emphasis on the problems associated with their practical implementation, and also gives a useful bibliography of other reviews, market surveys and conference proceedings.

1.4.2. STC Fibre Optic Sensor Systems

The sensor system which has resulted from the conceptual design activity associated with this contract phase is summarised schematically in Fig. 1. The system is based on two different types of fibre optic sensor. The first type, for temperature, pressure and status indication, is based on frequency-out microengineered silicon devices. The second type, for smoke detection, is based on a scatter cell. A sensor interface device (SENSID) is used for providing the optical input to the sensors and for processing their output. The sensor information is transmitted via a RS232 optical link to a systems interface device (SYSTID).

Techniques for the anisotropic etching of single crystal silicon to yield complex three-dimensional structures have been developed by STC at STL, Harlow, and by others, over a number of years (Ref. 16, 17 and 18). The use of these structures in transducers has been proposed by a number of workers (Ref. 19, 20, 21 and 22).

The silicon sensor at the heart of this work is based on a miniature mechanical resonator whose resonant frequency can be modified by the application of an externally induced strain. This enables a common sensor element, and the same type of optical inputs, outputs and signal processing, to be used in the construction of different transducer types. The individual transducer design for a required application is then achieved by the incorporation of an appropriate transduction mechanism.

Section 2 of this report provides a detailed analysis of the factors affecting the design of the common optical module and of the transduction mechanisms. Possible schemes for multiplexing sensors are also considered there. Different possible options for the signal processing of the sensor output are then analysed in Section 3.

STC has developed an operational system for monitoring the presence of low levels of oil pollution in the ballast and bilge water discharged by tanker and cargo ships (Ref. 23 and 24). The system works by light scattering techniques and has been fitted to a large number of vessels. This, and other related experience, has provided useful background information for considering the design of a smoke detection system based on similar operating principles. Section 4 of this report considers such a system and includes an analysis of smoke characteristics, the scattering of light by particles and the resultant requirements for the scatter cell design.

Section 5 of this report gives a brief discussion of the telemetry and display aspects of the system, consistent with the emphasis of work required under this programme.

It is appropriate here to review the system choices for fibre type and operating wavelength. A wavelength of 850nm has been selected for the system because of the availability of inexpensive silicon detectors, based on proven technology, and also because high powered laser diodes operating at this wavelength are readily obtainable. The lengths of interconnecting cables are relatively short and so the optical attenuation of the fibre at this wavelength is unlikely to be a major factor. Standard 50/125 um multimode fibre is envisaged as being used in the system because of its availability and its suitability for use in expanded beam terminations. These system choices are not rigid and could be modified if necessary given the availability of suitable components.

2. OPTICAL SENSOR DESIGN

2.1 Introduction

This section considers the design of pressure, temperature and status sensors. These incorporate a common optical module, the design of which will be considered first. The design of the different transduction mechanisms required is then described followed by an analysis of the sub-system power budget requirements in order to determine the optimum multiplexing configuration.

2.2 The Common Optical Module

The common optical module is shown schematically in Fig. 2 and can be seen to consist essentially of a silicon oscillator mounted in the free space beam between two graded index lenses. Insertion loss through such an arrangement is dependent on the separation of the lenses (Ref. 25) and consequently this distance should be as small as possible: for our design this will probably be about 20 mm. A small (0.1mm) samarium cobalt (SmCo) magnet is fixed to the back of the silicon oscillator so as to allow interaction with the electromagnetic circuit (Fig. 3) which is also contained in the module. Infra-red light of 850nm wavelength, for which high power semiconductor lasers are available, enters the module from the left through a standard telecoms type 50/125 um graded index multimode optical fibre terminated in a Stratos demountable graded index (GRIN) lens. A parallel beam of about 1 mm diameter is formed, part of which is incident on the silicon paddle where it is reflected onto a silicon PIN photodiode.

The area of the incident beam intercepted depends on the multiplexing configuration selected (see section 2.4). For a parallel arrangement of sensors only the modulated part of the beam is required to enter the output GRIN lens so almost 100% of the incident beam can be intercepted. For a series arrangement of sensors sufficient light must get past the first oscillator to drive successive oscillators. In this case, only about 10% of the incident light would be intercepted.

The resulting current produced by the photodiode induces a magnetic field in the inductor. This field is conducted by the metallic glass strip, located around the silicon oscillator, and appears across the gap where it interacts with the field of the small SmCo magnet fixed to the back of the silicon paddle. Metallic glass and SmCo have been chosen because of their high permeability and magnetic energy density respectively. The paddle rotates, deflecting the light beam from the photodiode and stopping the current. As there is no magnetic field generated in this position, the torsion in the supports rotates the paddle back to its original position and the process starts again.

An oscillation of the paddle thus ensues whose angular frequency (ω') can be shown to be given by:-

$$W' = W^* [(1 + Y/W^2 JCR^*) / (1 + Y L/J R^*)]^{1/2} \dots\dots(1)$$

where W^* is the natural frequency of the silicon paddle in this torsional mode, Y is the mechanical damping coefficient, J is the mass moment of inertia and L , C and R^* are the values of the inductance, capacitance and inductor resistance respectively in the electrical circuit.

Equation 1 is derived in Appendix A and the derivation assumes that the magnetic coupling between the electrical and mechanical oscillations is weak.

The part of the light beam which is not intercepted by the silicon paddle is collected by a second GRIN lens and is fed into the output optical fibre, which is also 50/125 μ m graded index multimode. The proportion of the light beam passing the paddle also depends on the angle of the paddle to the beam so that, as the paddle oscillates, the output light is intensity modulated to a depth determined by oscillation amplitude and with the frequency of the oscillation.

The amplitude of oscillation depends upon the amount of light reflected by the silicon paddle onto the photodiode, the efficiency of the electrical circuit, and the magnetic coupling between circuit and paddle.

The optical power reflected onto the photodiode by the paddle in its rest position is given by:

$$P = RI'A' \cos u \dots\dots(2)$$

Where R is the reflection coefficient of the paddle (averaged over all polarisation), I' is the incident light intensity and A' is the illuminated area of the paddle at angle u to the beam (i.e. at its rest position). Given a conversion efficiency of X amps/watt for the photodiode, we thus obtain a diode current (i) of:

$$i = XRI'A' \cos u \dots\dots(3)$$

The magnetic field (B) between the poles of the metallic glass is proportional to this current (i), and the torque (t) on the silicon paddle is given by:

$$t = Bms \sin v \dots\dots(4)$$

Where m is the magnetic moment of the Si_nCo magnet fixed to the paddle at angle v (typically 90°) to the enveloping field (B).

This torque, produced by the magnetic circuit acting on the small permanent magnet attached to the rear face of the paddle, causes a rotation of amplitude C^* given by (see Appendix A)

$$C^* = t' [J^2 ([W^*]^2 - W^2)^2 + W^2 Y^2]^{-1/2} \dots\dots(5)$$

The analysis leading to Equation 5, and also Equation 1, assumes ideal simple harmonic oscillator behaviour and is only true for small values of C^* . For larger values higher order terms become significant leading to hysteretic behaviour which manifests itself as an undesirable optical power dependence of the resonant frequency (Equation 1). Experimentally, we find that amplitudes of less than about one degree do not exhibit hysteresis. Figures 4 and 5 show the behaviour which is observed experimentally for both small and large amplitudes respectively.

We therefore have an upper limit on the oscillation amplitude and can work back to determine the sizes of the modulated signal and of the drive power. Detailed calculations on this are given in Appendix B. This analysis leads to a power requirement of 1mW for a 0.5° oscillation amplitude. It is hoped to reduce this power requirement significantly by reducing the optical module size and by improving the reflectivity of the oscillator.

2.3 Transduction methods

The silicon torsional oscillator designed for this application (Fig. 6) is a force sensor. Force applied to deflect the oscillator cantilever results in a tensile stress S along the supports of the paddle. This stress is related to the natural angular frequency $\omega(0)$ of the oscillator by:

$$\omega(S) = \omega(0)[1 + SJ^*/KG]^{1/2} \dots\dots(6)$$

where G is the shear modulus and K , the torsional stiffness constant, and J^* , the polar moment of inertia, are related to the dimensions of the paddle supports (Ref. 26).

Rearranging Equation 6, the value of S can be determined for a given change in natural frequency. It will be shown later (see Section 2.4) that a full scale change of 5% in frequency is desirable. The variation in the resonant frequency of the silicon sensor with the force applied to the cantilever has been investigated experimentally and a 5% change in frequency has been demonstrated (Fig. 7). Using typical values for J^* , K and G (Appendix C), we obtain a value of 14 Nm^{-2} for S for a 5% change in frequency.

For a cantilever, the force D required to produce a stress S in the surface of the cantilever under tension is given by (Ref 27 and 28) -

$$D = SI/xz \dots\dots(7)$$

where I is the moment of inertia of the cantilever section, x is the distance from the point of application of the force to the position at which S is measured (ie. the oscillator) and z is the distance of the surface under tension from the neutral axis (i.e. half the cantilever thickness). Again using typical values (Appendix C) and S equal to 14 MNm⁻², we obtain a value of D for a 5% frequency change equal to 0.22N.

For the measurement of temperature a bimetallic strip would be caused to act on the cantilever. Supposing that a full scale range of 100°C is required then the force produced by the bimetal strip must be approximately equal to the 0.22N required to produce 5% change in frequency. The force F' developed by a restrained bimetal cantilever subjected to a temperature rise T* is given by (Ref. 29).

$$F' = a'b's^2ET*/4l' \quad \dots\dots(8)$$

Where a' is the specific thermal deflection, b' is the strip width, s the thickness, E its modulus of elasticity and l' its length. Typical data from manufacturers suggest that a' = 20.8 x 10⁻⁶ °C⁻¹, b' = 1 mm, s = 0.25 mm, E = 1.35 x 10⁵ N mm⁻² and l' = 20 mm. Hence, for T* = 100°C, F' = 0.21 N.

The bimetallic strip may be arranged in the optical module to act directly upon the silicon cantilever in which case precise matching of the forces can be achieved by adjusting the point on the cantilever to which the force is applied. However, unless the optical module is very small the thermal time constant of the sensor will be large. It may then be preferable to have the bimetal outside the optical module and apply force to the cantilever indirectly using a torsion tube (Fig. 8). A torsion tube is simply a thin walled cylinder, with a low resistance to twisting, with a rod down its centre and welded to the cylinder at one end. Thus rotary motion can be transferred into a sealed box via the rod without using sliding seals. The thermal time constant is determined by the thermal mass of the bimetal in this case, and fine adjustment of the forces can be achieved by adjusting the lever lengths attached to the ends of the rod.

The force required to deflect a torsion tube (Ref. 30) of typical dimensions (inner diameter 1.8mm, outer diameter 2.0mm, length 20mm) made of brass (shear modulus G = 3.73 x 10⁴ Nmm⁻²) is considerably larger than that required to deflect the silicon cantilever so that the predominant part of the design involves matching the force generated by the bimetal to that required to twist the torsion tube. If the restrained (i.e. zero deflection) force for a bimetal cantilever is F' (Equation 8) and the free deflection is A, then the force (F*) generated due to a partially restrained bimetal is:

$$F* = F' (1 - d/A) \quad \dots\dots(9)$$

where d is the allowed deflection. If we assume that d = A/2 then F* = F'/2, or using Equation 8 -

$$F^* = a'b's^2ET^*/8l' \quad \dots\dots(10)$$

Such a deflection d applied to a lever of length g would cause a rotation of angle $y = \arcsin(d/g)$. For our purposes, this is likely to be small so we can make the approximation $y = d/g$, Given that:

$$A = a'T*(l')^2/s \quad \dots\dots(11)$$

and that the torque t required to cause a twist y in the tube is:

$$t = \pi[c^4-r^4]Gy/2l \quad \dots\dots(12)$$

Where l is the tube length and r and c are the inner and outer tube radii respectively, the force required to be applied to the lever of length g to produce this torque is t/g and becomes:

$$F'' = (\pi)(c^4-r^4)Ga'T*(l')^2/4slg^2 \quad \dots\dots(13)$$

Where substitutions for y and t have been made in (12) using (11). As F'' is produced by the bimetal it must be equal to F^* so that setting Equation 10 equal to Equation 13, we obtain a relation between the various components of the system:

$$b's^3 = 2(\pi)(c^4-r^4)G(l')^3/Elg^2 \quad \dots\dots(14)$$

Appropriate values to satisfy Equation 14 are $b' = 2.4\text{mm}$, $s = 0.5\text{mm}$, $l = 20\text{mm}$, $c = 1.0\text{mm}$, $r = 0.9\text{mm}$, $g = 10\text{mm}$. In this case, $F^* = 9\text{N}$ which is much greater than the 0.22N required to bend the silicon cantilever so the latter does not invalidate the above calculations.

For the measurement of pressure an evacuated bellows can be caused to act on the cantilever via a torsion tube in a similar manner to the bimetal strip. In this case, let us assume that full scale is 1 atmosphere (10^5Pa). For a bellows of effective area A^* the force produced by an external pressure p is given by:

$$F = pA^* \quad \dots\dots(15)$$

Manufacturer's data (Ref. 31) suggests $A^* = 4 \times 10^{-5}\text{m}^2$ so that for $p = 10^5\text{Pa}$ a force of 4 N is generated. This force is again much larger than the 0.22N required to deflect the silicon cantilever so that the primary design criterion is to match the deflection of the bellows to the rotation of the torsion tube. The deflection d of a bellows of spring rate k subjected to a force F is given by:

$$F = kd. \quad \dots\dots(16)$$

The deflection of a lever of length g attached to a tube of length l and inner and outer radii r and c and shear modulus G is related to the applied force F'' by:

$$F'' = (\pi)(c^4-r^4)Gd/2lg^2 \quad \dots\dots(17)$$

where, as in Equation 13, the angular deflection y has been approximated by d/g . Setting $F = F''$ we obtain:

$$g^2 = (\pi)(c^4 - r^4)G/2lk \quad \dots\dots(18)$$

Suitable values are $c = 1.0\text{mm}$, $r = 0.9\text{mm}$, $G = 3.73 \times 10^4 \text{Nmm}^{-2}$ (brass) $l = 20\text{mm}$ and $k = 11.7 \text{Nmm}^{-1}$ giving $g = 9.2\text{mm}$. These values are similar to those for the temperature transducer so leading to commonality of components.

The isolation of the measurement medium from the optical module by means of a torsion tube conveys the advantage that the optical module may be sealed, by for instance a PVC dip coating, thus preventing the ingress of contaminants and allowing the total immersion of the transducer.

In both the temperature and pressure transducers overrange protection of the silicon cantilever can easily be achieved by positioning a stop behind it, or alternatively by causing the zero position to correspond to maximum strain so that increasing the measurand reduces this strain until at full scale the lever leaves the cantilever altogether. Clearly alternative temperature and pressure ranges can be achieved by suitable choice of bimetal or aneroid bellows.

The status sensor can be configured in several ways. Where small movements of the device whose status is required to be determined are involved, the device may act directly or via a suitable lever or gear onto the torsion tube lever, as for the pressure or temperature sensors. Typical movements of this lever are less than 1 mm. Alternatively, the configurations shown in Fig. 9 may be used. In Fig. 9a the shutter interrupts the output beam so that in one position no signal is obtained and in the other a modulated signal at the frequency of the silicon oscillator is output. However, failure of the light source simulates the no output position. Both 9b and 9c avoid this situation by having two oscillators at different frequencies. Thus, the receipt of one frequency indicates state 0 and the other state 1. However, both 9b and 9c require twice the optical power of 9a. Although 9b requires additional components compared to 9c, it has the advantage of maintaining both oscillators in motion at all times so improving response time. (9c has a dead space of approximately 1s while the oscillation builds up).

2.4 Multiplexing

The number of sensors that can be multiplexed onto a single optical fibre is limited by two constraints. Firstly, the frequency bands occupied by individual sensors must not overlap if ambiguities are to be avoided and secondly the power available from the driving laser must be sufficient. The bandwidth requirements will be considered first.

The larger the number of multiplexed sensors, the smaller the bandwidth that can be occupied by each, thus limiting the resolution of each sensor. In addition, harmonics of the lower frequencies must not fall in the higher frequency bands (Ref. 32). The choice of frequencies therefore lies between the set of odd numbers (1, 3, 5, 7, ...), such that all intermodulation frequencies appear as the set of even numbers (2, 4, 6, ...), or, alternatively, a set within one octave (1 to 2), such that intermodulation frequencies fall between 0 and 1. The requirement to limit the variation in silicon oscillator dimensions leads us to choose the second alternative.

The number of sensors which can be multiplexed within one octave is then determined by the resolution required and the uncertainty in the measurand due to errors in oscillation frequency. The dominant cause of error in oscillation frequency for a given value of measurand is the temperature coefficient of the sensor (Appendix C). This is related to the bandwidth (W''/W) required by each sensor and the operating temperature range T^* by:

$$W''/W = (T^*/RW) W/ T \quad \dots\dots(19)$$

Where R is the resolution required for a given sensor as a fraction of full scale, W is the base angular frequency, W'' the full scale change in angular frequency and $1/W(W/ T)$ is the sensor temperature coefficient.

TABLE 1.
Normalised frequency bands of 5% width fitted within one octave.

Band (Sensor number)	Normalised Frequency Range
1	1.00 - 1.05
2	1.09 - 1.15
3	1.19 - 1.25
4	1.30 - 1.37
5	1.42 - 1.49
6	1.55 - 1.63
7	1.70 - 1.78
8	1.85 - 1.94

Typically we might expect to achieve a temperature coefficient of 50 ppm/°C over a temperature range of 10°C. Thus for a resolution of 1% a bandwidth of 5% is required by each sensor. Table 1 lists eight normalised frequency bands of 5% width fitted within an octave whilst allowing space between adjacent bands to reduce any possibility of overlap due to manufacturing tolerances or signal processing limitations.

In order to extend the temperature range over which the 1% accuracy can be achieved the temperature at the sensor must also be measured (by a silicon sensor suitably configured with a bimetal strip) and compensation made in the processing. Thus a pressure sensor would effectively occupy two sensor frequency bands.

The second constraint on the multiplexing of sensors is the available power from the driving laser which must be greater than the sum of the drive powers required for the individual sensors and the losses through the optical system. This sum is strongly dependent on the arrangement of the sensors, three variations of which are shown in Fig. 10, 11 and 12.

In the series arrangement (Fig. 10) the lowest incident power occurs for the sensor furthest from the laser and is determined by the insertion loss per sensor and the number of sensors. The cable loss is likely to be small over the likely distances involved. In the parallel arrangement (Fig. 11) equal power arrives at each sensor, determined by the insertion loss of the couplers between the sensor and the laser. Combinations of series and parallel arrangements are also possible. If the insertion loss of each sensor is small compared to that of a coupler then the total power required by the series arrangement will be lower than for the parallel configuration. In our case, we predict a loss of - 5dB per sensor and an excess loss of - 1dB per (1:2) 3dB coupler. (A 1:4 coupler is equivalent to two 3dB couplers in series, and so on). As a result, the parallel arrangement requires considerably less power than the series arrangement: + 12dB relative to the minimum sensor drive power for the parallel arrangement compared with + 35dB in the series case.

Experimentally, we have found the minimum sensor drive power to be approximately 1mW giving a total power requirement of 16mW for the parallel arrangement and 3W for the series configuration. The latter power requirement is not feasible using currently available semiconductor lasers, even if an improved efficiency could be obtained by coating the silicon to improve its reflectivity.

The preferred configuration is therefore the parallel one (Fig. 11), which also confers the advantage of graceful system degradation in the event of a sensor failure. A further possibility is that the sensors may be operated in parallel, reflective mode (Fig. 12) by replacing the output GRIN lens with a mirror. This has the additional advantage that only a single fibre cable has to be connected to the sensor.

3. SIGNAL PROCESSING

3.1 Introduction

The signal processing section in the SENSID unit is required to transmit the value of the measurand at each sensor to the system interface device. The preceding section has described the nature of the sensors for the measurement of temperature, pressure and status. It has been shown that up to eight silicon oscillators may be multiplexed together and that the frequency outputs span an octave, having individual frequencies of around 1kHz.

A full scale change in measurand results in an oscillator frequency change of 5%. For a resolution of 1%, a frequency recognition resolution of better than 0.5Hz in 1kHz is required. The frequency signal must be obtained in such a form that it can be input directly to a computer for further processing.

The light power levels from the sensors will be of the order of tens of microwatts and the modulation depth of the signal will be of the order of a few microwatts.

A schematic diagram of the signal processing is shown in Fig. 13. The signal processing will be considered here in three sections: pre-processing, demultiplexing and computer interface. The demultiplexing section has formed the main area of study and has been looked at in two parts, digital and analogue methods. It will be shown that an analogue method, using phase lock loops (PLL), offers the preferred approach to demultiplexing.

3.2 Pre-processing

The signal pre-processing is shown in Fig. 13 in simplified form. The optical signal is detected by a silicon photodiode (eg. type BPX 65 or equivalent) and the electrical signal is converted to a voltage by means of a transimpedance amplifier using a low noise operational amplifier (eg. type OP27). The small capacitor, C_1 , prevents parasitic oscillation of this stage and also reduces the effects of signal harmonics. The frequency response of this section should not be a problem and the slew rate would be the limiting factor with a very high feedback resistor. Generally 1/f noise is a function of the feedback resistor and the open loop gain of the amplifier. AC coupling to the next stage will reduce the amount of 1/f noise and this may be accomplished with the capacitor, C_2 .

3.3 Demultiplexing

The demultiplexer must take the signal from pre-processing and turn it into eight separate logic level signals corresponding to the frequencies of the multiplexed sensors.

3.3.1 Digital methods

A digital approach to demultiplexing first requires the use of an analogue to digital convertor. An eight bit analogue to digital converter is commonplace and an example for use in the system would be the Ferranti ZN439E-7 which has a conversion time of five microseconds.

Three alternative implementations of a digital demultiplexing algorithm have been considered:

- (i) A very large scale integration (VLSI) device could handle an algorithm having the potential for high speed operation. However, no such device has been found to be available and a customised device would be prohibitively expensive.
- (ii) A computer interface card, performing much the same process as the VLSI device, has similarly not been found.
- (iii) A computer program performing a Fourier Transform is an obvious and desirable solution. When adapted to the computer the process becomes the Fast Fourier Transform (FFT) and an analysis of the timing and memory requirements of this approach has been made.

For the resolution required, about 100,000 computer operations per second would be required and this would take about one minute on the 2 MHz processor envisaged for the system. Use of the fastest readily available computer (which runs at 16 MHz) still gives a long time requirement of about seven seconds for the computation. Such a computer would also be very expensive. An alternative approach, using look-up tables instead of performing the multiplications and additions associated with the computation, would reduce the time requirement to less than one second. However, a further time limit is imposed by the sampling time which, for the frequency range and resolutions required, would be of the order of one second.

The memory required for the computations would be 1600 squared bytes, i.e. 2.5 Mbytes.

The FFT approach to signal demultiplexing has not therefore been found to be attractive because of the long processing time and large memory requirements.

3.3.2 Analogue Demultiplexing

Introduction

The requirement for analogue demultiplexing is to take the single output from the optical detector, discriminate between the channels contained within, and present each of these in a logic compatible form to the microcomputer interface. Three alternatives for performing this task have been considered, and each is discussed in this section. The relative merits and disadvantages of each method are examined.

The proposed technique is then considered further, with any problems expected to be associated with it being highlighted.

Band Pass Filters

A set of high Q band pass filters, one for each sensor in the multiplexed loop was considered. The signal from the detector circuit would be divided 'n' ways, where n is the number of sensors. Thus the same signal is fed to each of the n filter circuits (see Fig. 14(a)).

The centre band frequency of each filter is designed to be equal to the nominal centre frequency of its associated sensor, and the filter bandwidth depends on the range of frequencies that the sensor can output. The filter characteristic should therefore be flat across the passband, rolling off sharply so that frequency components in adjacent sensor channels are heavily attenuated. The desired channel frequency that is passed by the filter must then be conditioned to provide a suitable digital signal to the microcomputer interface.

However, it is expected that the guard bands between channels will be very narrow (about 20 Hz) for channels in the range of 400-800 Hz. Implementation would need very high Q filters to give the necessary rejection, which would result in a non-flat passband. Such discrete filters would require a considerable number of components and hence poor reliability and temperature stability could be expected. This type of solution is considered as being neither suitable nor practical for this application.

Intermediate Frequency Filters

This technique employs a heterodyne principle to mix the signal frequencies up to an intermediate frequency (IF) band, where a single high quality tuned filter would be used to discriminate between channels; Fig. 14(b) shows the scheme. The local oscillator (LO) has 'n' preset frequencies where n is the number of sensors multiplexed. Each value is $(IF + f^*)$ where IF is the chosen intermediate frequency and f^* is the nominal centre frequency of the ith sensor. The input signal is mixed with the LO output, the mixer generating sum and difference terms for each sensor channel with the LO. Only the channel corresponding to the current LO setting will be passed by the filter, whose centre frequency equals the IF, all others being attenuated.

This signal is then translated back to the baseband using a second mixer and a low pass filter.

This technique has the advantage that the processing takes place in one frequency band, and so only one filter is needed, albeit of high tolerance and stability. However, several disadvantages have been identified:-

- the method requires either 'n' oscillators or possibly a presettable synthesizer.
- output conditioning is needed.
- simultaneous outputs from all channels are not possible; some scanning system would be required.

Phase Lock Loops

The Phase Lock Loop (PLL) can be considered as a narrow band tracking filter, that locks on to the desired input signal and reproduces it as a logic-compatible square wave output, exactly equal in frequency. This function is available on a single, low-cost integrated circuit (IC) and it is comparatively simple to set up the required operating conditions.

One device is needed for each sensor. Each device is configured initially to capture a specific sensor output and then remain locked to it as the measurand causes its resonance to vary. Such a scheme demands little hardware and is shown in Fig.14(c).

The narrow bandwidth of the loop results in high rejection of noise at the input. This is an important feature in this application where there are many potential error or noise sources caused by temperature effects, ageing, coupling losses, maintenance alterations etc.

Therefore, for reasons such as low cost, low component count, functional simplicity, high noise rejection and design flexibility, it is proposed that using phase lock techniques provides the most suitable method for the demultiplexing aspects of the signal processing.

PLL Considerations

Fig. 15 shows the format for the distribution of channels and the constraints for the design of the PLL receivers. The PLL capture range must extend across the total frequency deviation for that sensor, so that on power-up the receiver can lock on to the sensor output irrespective of its current resonant state. The channel bandwidth is defined as the total sensor deviation plus 50% of the guard band on each side. The capture range must therefore be less than the channel bandwidth in order to avoid false locking to an adjacent channel. It is proposed to set the limits of the capture range between these two boundary conditions so that frequency drift in the PLL voltage controlled oscillator (VCO), as a result of temperature variation, does not violate these criteria.

Estimates can be made to determine operational requirements with respect to temperature based upon PLL VCO drift. If we assume that the width of the capture range remains constant, but that it is shifted due to temperature induced changes in the VCO, a worst case condition can be calculated:

Temperature co-efficients:

VCO	$\pm 0.03\% / ^\circ\text{C}$	(from + 25°C)
Frequency setting, R & C components	$\pm 0.014\% / ^\circ\text{C}$	
TOTAL	$\pm 0.044\% / ^\circ\text{C}$	(440ppm/°C)

For sensors with a 5% fullscale change centred at around 400 Hz and with a 20 Hz guard band, it has been calculated that the PLL electronics must operate within the range +5 to +45°C if the boundary conditions are to be maintained. This is an operational requirement that will have to be carefully addressed during development.

The circuit response time for the PLL has been analysed and depends on the time constant of the PLL low pass filter. This may be estimated by reference to design curves (Ref. 33).

It can be shown that the governing filter time constant, T is given by

$$T = k/W^2 \text{ seconds}$$

Where k is the PLL oscillator lock range (rad. s⁻¹) and W is the loop natural frequency (rad. s⁻¹).

A figure of merit for a PLL is defined as

$$F = \frac{\text{capture range}}{\text{closed loop bandwidth}}$$

The denominator is the total sensor deviation in this application.

Assuming a sensor frequency deviation of 20Hz, and a capture range (W^*) extending past this by 25% of the 16Hz guard band on each side (refer to Channel multiplexing scheme, Fig. 15) then

$$F = \frac{28}{20} = 1.4$$

From design curves, this gives:

$$W/k = 0.46$$

and

$$W^*/k = 0.5$$

With the capture range, W^* of 28 Hz,

$$k = 352 \text{ rad.s}^{-1}$$

and

$$W^* = 160 \text{ rad.s}^{-1}$$

Thus,

$$\text{Filter time constant, } T = \frac{352}{160 \times 160} = \underline{14 \text{ ms}}$$

It is therefore estimated that the output will follow a step change in the input frequency with a delay of the order of fourteen milliseconds.

The PLL's ability to lock on to signals buried in noise can be enhanced if a limiting circuit is employed ahead of the PLL input. This has the effect of eliminating noise associated with amplitude variations in the input signal. Some commercial PLL devices include a limiting stage prior to the phase detector on the chip, thus further simplifying hardware design.

Appropriate alarm circuits would be included in the design to give an indication of signal failure by detecting an out of lock condition for the PLL.

Two integrated PLL devices have been identified and both are readily available and similarly of low cost. Although they have essentially the same circuit block, differing features exist between them, due primarily to the technology used: the LM565 is a linear device whereas the 4046 is CMOS. A test programme to determine overall device suitability is proposed.

3.4 Computer Interface

The demultiplexed signals, now at logic level and discrete (one signal per sensor) will be selected, one at a time, for transmission to the computer for further processing. Before they arrive at the computer, however, they must be turned into bytes of data that the computer can understand. The computer must be able to address each sensor and receive data concerning the measurand.

An interface card has been designed and built under STC p/v funded activity and this gates pulses from a 16.532548 MHz crystal with the signal inputs. The result from this is sent through a 16 bit counter, registered and transmitted to the microprocessor. The count of gated clock pulses is directly proportional to the sensor frequency.

A resolution of 0.5Hz in 1kHz is necessary and so the minimum clock frequency is given by -

$$\begin{aligned} \text{Minimum clock frequency} &= \frac{\text{Sensor frequency} \times \text{Sensor frequency}}{\text{Sensor resolution}} \\ &= 2\text{MHz} \end{aligned}$$

The crystal used has been selected from a standard range having a low temperature coefficient.

The interface card will send 8 bit data bytes to the computer through a programmable read only memory (PROM). This memory contains conversion and linearisation constants for the individual sensors. If a sensor is replaced then the appropriate linearisation PROM will also be replaced. The 8 bit data byte will be used as an address in the PROM and the data contained at that address will be sent to the computer. Thus no electronic intelligence is required in the SENSID unit.

Work will be required to enable the eight phase lock loops to be connected to the front end of this interface card. It is intended to feed the output to a CUBE industrialised personal computer. This incorporates a 6502 based processor and will be programmed in a high level language (Basic).

The computer then turns the number into a figure in units of the measurand. The time taken for this operation has been assessed and a worst case estimate is 16.3 milliseconds.

4. SMOKE DETECTORS

4.1 Introduction

The need for an effective smoke detector has already been considered under the review of conventional sensor systems (see Section 1.2). This has shown that there is no effective smoke detector available for use by the USN. This section considers the design of a smoke detector operating on light scattering principles.

The basic requirements for a smoke detector may be summarised as follows (Ref. 34):-

- (i) The earliest possible alarm of the emission of smoke from a fire must be given. Circuits in either the detector or the control equipment for the prevention of false alarms must not interfere with the operation of the system but must also be adequate to prevent false alarms.
- (ii) Detectors must operate reliably under the environmental conditions appropriate to where they are installed. Factors such as changes in ambient temperature, relative humidity and light intensity must not affect the operation of the detector.
- (iii) Detectors must be resistant to adverse long term environmental factors such as corrosion, vibration and the accumulation of dirt.
- (iv) In the time period between planned maintenance of the detector, the threshold value for alarm must keep within a range such that adequate sensitivity is ensured without the detector being prone to false alarms.
- (v) The detector may be sited in areas where discrimination from other air-borne materials is required. For example, exhaust fumes, steam or paint vapours may be present.

4.2 Smoke characteristics

Reference is made here to the particulate components of the combustion products, rather than the gaseous ones, since light scattering only operates on particles. The two most important aerosol properties affecting the performance of scatter based detectors are the concentration of the smoke and the particle size. There is a lack of quantitative data regarding the dependance of smoke detector performance on these factors because of the difficulties involved in reproducibly generating a smoke aerosol of fixed size, coupled with the complex measurement problem of characterising the aerosol (Ref. 35).

The size distribution of the aerosol changes as a result of the phenomenon of particle coagulation for recirculating generators. Small scale experiments with flaming Douglas Fir, polyvinylchloride and rigid urethane foam indicate that the peak particle size in terms of mass size distribution under smouldering, or pyrolysing mode, are 0.5 to 1.5 micrometres. After the initial stages of fire, the particle size range decreases to 0.1 to 0.3 micrometres. A scatter detector may be expected to be sensitive to particles having a size down to 0.1 micrometre (Ref. 35).

A useful summary of particle sizes is given in Fig. 16 and this diagram has been derived from a table given in Ref. 36. This shows that most smokes span a size range of 0.01 to 1 micrometres.

Indoors, smoke rapidly rises from a fire in a thin column, widening and entraining air as it does so. As it loses heat and meets resistance from upper, warmer layers of air it mushrooms out in a turbulent fashion. At the height where the temperature of the smoke is the same as that of the air, it will stop rising until increased fire activity provides more energy to drive the smoke further upwards. To detect smoke in some circumstances it may be necessary to install sensors in several places (Ref. 37).

4.3 Methods of Smoke Detection

There are several possible methods of sensing smoke and the most commonly used of these is the Ionisation type of detector. A simplified version of this detector is shown schematically in Fig.17. A small radioactive source, which is frequently Americium, is used to ionise the test air to produce positive and negative primary ions (Ref. 35). The interaction of these ions with test particles is used to generate a current which may be amplified and displayed or used to generate an alarm.

Another method of smoke detection is by the use of light. A simple attenuation of light between the emitter and the detector may be used but this suffers the drawback that any obstruction in the optical path will attenuate the signal. Many sources of attenuation could therefore be misinterpreted unless the application is very well characterised. Particle size discrimination is also not possible and no allowance can be made for the fouling of optical surfaces.

Neither of the above methods is suitable for the present application.

4.4 Light Scattering

An alternative optical method is based on the detection of the light scattered by smoke particles and this is shown schematically in Fig. 18.

The angle of scatter is related to the particle size and shape and to the wavelength of the incident light. The intensity of scattered light is related to the concentration of smoke particles present. There are limits to the range of particle sizes that may be observed by scattering arising from the physical effects of light scatter.

If the particles are much larger than the wavelength of the incident light, reflection will occur and the direction will depend on the orientation of the irregularly shaped smoke particle, as follows from geometrical optics.

If the wavelength of light is much greater than the diameter of the particle, Rayleigh scattering will occur. This is mostly scatter with a very low absolute intensity. There are intensity maxima in the forward and reverse directions and there is a minimum in the plane of symmetry.

As the radius of the sphere is increased from the Rayleigh regime there is a departure from symmetry, more light being scattered in the forward direction than backwards. This phenomenon is called the Mie effect. When the light wavelength and the particle diameter are similar in size, Mie scattering occurs. Here diameter changes with fixed wavelength will have a large effect upon the output at different angles and analysis of the intensities at two angles will afford the concentration of particles of a particular diameter. This particle size discrimination is not possible under the other scattering regimes where the particle size is much greater or much smaller than the wavelength of the light.

The wavelength of the light, which in our case is 850nm, should ideally be of the same order as the particle diameter. A detailed analysis of Mie scattering involves lengthy and complex mathematical formulae (Ref. 38) and this analysis may fortunately be reduced to a simplified relation which is used to given the diagrams shown in Fig. 19 (Ref. 39). A parameter q is used, defined by

$$q = 2(\pi)a/w$$

where a is the particle radius and w is the wavelength of the incident light.

For particles having radii from 0.005 to 0.5 microns, the value of q ranges for 0.02 to 2.0. The polar diagrams in Fig. 19 show a plot of scattered light intensity at different angles, for the perpendicular and parallel polarisations, at different values of q . For small q , the polar diagrams are symmetrical about the plane through the centre of the sphere, at right angles to the direction of propagation of the light. At high q values, the intensity of the scattered light has an angular dependence. By detecting the intensity of the scattered light at two scatter angles, 10 and 30 degrees would be appropriate choices, it would be possible to determine the concentration of selected particle sizes. An experimental programme would be required in order to do this.

4.5 Scatter Cell Design

The proposed scatter cell would be a simple, robust single piece casting into which standard communications fibre connectors and beam expanders would be screwed. The design is shown schematically in Fig. 20.

The emitter and two scatter detectors have expanded beam connectors in order to cut down the amount of light which could be reflected off the cell walls and to improve the definition of the scatter angles. The detectors would collect scattered light from an area located at the centre of the cell, and other light arising from second and higher order scattering. The sensitivity of the sensor would therefore be enhanced if the smoke could be channelled into this central area. This may be difficult to implement without electrical power.

The two angle detection system proposed here has been used in a land based version of the oil in water monitor referred to in Section 1.4.2. The two detector outputs were used to compute two concentrations, one for oil and the other for solid particles. The particle sizes of each component were known and this information was used to derive an algorithm for use by a microprocessor. The system has been shown to detect zero to two parts oil per million parts water and also zero to two parts per million solids. A crosstalk, between the two concentration measurements, of less than 1% and a resolution of less than 0.01 ppm have been realised. A direct, straight through beam was used to provide compensation for fouling of the optical surfaces and degradation of the components. There is therefore good precedent that a scatter cell of this type can be used in a discriminating way.

A development programme would be required to investigate the response of the cell to differently sized particles, to determine if a baffle is needed in the cell to shield the scatter detectors and to examine cell window fouling. Further development could produce a cell having a reduced fibre connection requirement by the use of novel multiplexing techniques.

4.6 Smoke detection systems aspects

A schematic diagram for the system is shown in Fig. 21. The optoelectronics and signal processing would be located in the SENSID unit which would be connected to the scatter cell by an optical fibre cable and to the SYSTID unit by an RS232 link.

A microprocessor in the SENSID would send timed pulses of defined current amplitude, through a digital to analogue port and current booster, to the laser drive. The detector output signals would be multiplexed into an analogue to digital convertor, via preamplification, and operated on by the microprocessor. The preamplifier would use phase sensitive detection for maximum noise rejection.

The direct beam would be read and compared to a preset, reference level and the laser power adjusted to equalise the two values. This would constitute an automatic gain control and at maximum allowable gain an alarm could be initiated.

The scatter signal would be operated on by an algorithm which had been pre-loaded with coefficients appropriate for the application. The coefficients could be altered to suit changing conditions, ie they could be adaptive.

The optical losses in the system have been analysed and the results are shown diagrammatically in Fig. 20. System losses, excluding those associated with "straight through" attenuation or scattering, have been estimated at 14dB. A "straight through" loss of 10dB has been estimated giving a total direct loss for the system of 24 dB. The loss due to scatter is difficult to estimate because of lack of knowledge of the concentration of particles in smoke. Reference to other work in oil in water detection suggests that an equivalent smoke concentration of 100 ppm may be appropriate (Ref. 40), in which case an additional scatter loss of 20dB should be included.

Consideration of the detector sensitivity then leads to a requirement for a 5mW laser. In practice, this power requirement could be reduced by the use of phase sensitive detection, which reduces the noise bandwidth but also increases the time taken to process the signal.

5. TELEMETRY AND DISPLAY

5.1 Introduction

Telemetry is required to transfer sensor information (address, data, and data units) from the sensor interface device or devices to the system interface device where all information is collated and displayed. The basic telemetry requirements are for compatibility with the microcomputers used at either end of the link, and for the data to be transferred from each SENSID every ten seconds without degrading overall system performance. The latter implies that the data be transferred at as high a rate as is practical, to avoid impinging on the processing time required at a SENSID for other tasks (polling individual sensors, data storage, and data display, for example).

Consideration of the problem resulted in the choice of an RS-232C link, as this is most easily implemented in both electrical and optical form, and is a common industrial standard. An asynchronous link also avoids the need for a common clocking between any of the sensor or system interface devices, and provides some measure of graceful system degradation - if a sensor interface device fails, the rest of the system remains intact. It is anticipated that system interface devices will be receivers only and do not poll. This will allow duplication of SYSTIDs.

5.2 Telemetry

To ensure system operation, within the ten second time slot, an analysis of information protocol was conducted, with the following inputs:

- Sensor resolution of 1/256 (ie 8 data bits)
- A maximum of 256 sensors per sensor interface device (8 data bits)
- RS-232C protocol at a bit rate of 4800, 9600, or 19200 bits/sec. This last rate is not guaranteed on the chosen microcomputer. Information will be carried as ASCII characters.

RS-232C protocol requires one start bit, a choice of seven or eight data bits, one parity bit (optional but desirable), and one stop bit. Therefore, there are eleven bits per word (eight data bits are needed) and three words are required per sensor - one each for address, data, and engineering units/alarm levels. These three words will be transmitted every time the sensor interface device transmits data. A total of 33 bits are then required for each sensor, giving 8448 bits for 256 sensors. The time taken to receive data from a sensor interface device is then 1.76, 0.88, and 0.44 seconds at the different bit rates. For the demonstration system, 0.88 seconds gives sufficient time for the other computer activities within a ten second time slot, and a rate of 9600 bits/sec is therefore chosen. This also allows multiple sensor interface devices to be used with a single system interface device.

Note that the data transfer protocol is not restricted to an asynchronous RS-232C link, but has been selected for convenience and ease of implementation, as a support activity for the overall programme.

There are several suppliers of full duplex RS-232C optical links, each of whose systems will allow for simple insertion into a 9600 bits/sec electrical asynchronous path with minimal power supply requirements, and with transmission path lengths up to 1500m as standard.

5.3 Display

Sensor data will be output to a monochrome CRT display in alphanumeric mode. The system interface device will decode sensor information - for system flexibility and expansion all individual sensor identification will be resident in each set of signal processing electronics. No system interface reprogramming will be required if sensors are added or removed.

The output format for the demonstrator will be sensor address, type, reading, units, and alarm (audible as well as visual, if required) when a preset alarm level has been reached. The display will scroll, but operator intervention will allow particular sensor data to be displayed.

Flowcharts for the programs associated with the operation of the SENSID and SYSTID units have been devised and are shown in Figs. 23 and 24 respectively.

6. CONCLUSION

Introduction

The conceptual design of a fibre optic sensor system for the measurement of pressure, temperature and status and the detection of smoke has been described in this report. With the exception of the smoke detector, the sensors are based on a common optical module containing an oscillating silicon paddle. The oscillation frequency of the paddle is varied by interaction with the measurand.

The pressure sensor uses an evacuated bellows to apply force to the silicon oscillator via a torsion tube. The temperature sensor uses a bimetallic strip for applying this force. In the status sensor, force may be applied directly to the torsion tube or, alternatively, a shutter could be arranged to interrupt the output signal. Different ranges for these sensors may be achieved by varying only the bellows or the bimetallic strip as appropriate.

Experimental work, conducted under another programme, has provided a successful laboratory demonstration of the operating principles of the common optical module.

System advantages

The advantages of the sensor system may be considered in two parts. Firstly there are advantages, which are widely recognised, associated with fibre optic systems in general. Secondly, there are advantages which are specific to this sensor type and these will be highlighted here.

The sensors operate by the measurement of frequency, as opposed to amplitude, changes. The sensors will not therefore be adversely affected by a whole range of possible changes in other parts of the system. These system changes could arise from variations in source output, for example as a result of device ageing or temperature effects, and in attenuation changes in the interconnecting cables and connectors. The latter changes could arise for a variety of reasons, for example system repair or reconfiguration, microbending effects and temperature effects.

The sensors in multiplexed form offer significant potential flexibility in the way that they can be configured for use.

The sensor method is potentially capable of high sensitivity and accuracy, although there will be balancing trade-offs with multiplexing capability and this aspect is discussed further below.

The sensor design has been approached in terms of considering general sensor capability, independent of particular application requirements. However, the sensors, with their digital output, could be envisaged as forming part of an advanced, integrated system for damage control and such a system could include the development of Expert Systems to assist USN personnel in dealing with incidents. The damage control aspect has therefore been included in this report so that potential, practical application requirements can be considered from an early stage of development.

Factors affecting further development

The next development phase, involving the detailed design, construction and testing of transducers having specified performance represents a significant step forward from the present state. The analysis made under this study has identified a number of key factors which will have to be considered carefully during further development.

Accuracy and temperature effects

It has been shown that there is a trade-off between the resolution, and accuracy, achievable for a single sensor and the number of sensors that can be multiplexed into a single optical link. This trade-off arises because the total bandwidth available for the multiplexed array of sensors is one octave, in order to avoid aliasing, and the accuracy with which the measurand can be determined depends on the drift in frequency of an individual sensor.

The sensor frequency drift will be dominated by the temperature coefficient of the sensor itself, provided that the processing electronics can be maintained in a reasonably temperature stable environment. The values derived indicate that, in the measurement of pressure, and possibly status, the temperature will also have to be measured if more than two or three sensors are to be multiplexed and a reasonable resolution is to be achieved. Reducing the temperature coefficient therefore represents one of the major risk areas in the development of a sensor system such as this.

Signal processing and time constants

Possible alternative techniques for signal demultiplexing have been considered and it has been proposed that a system using phase lock loop integrated circuits should be adopted. This method potentially provides the best operational performance and design flexibility at comparatively low cost.

In further development it will be necessary to evaluate some commercial devices to determine the most suitable. Factors such as noise performance, response time, temperature dependence and lock acquisition properties would be assessed.

The time constants for the sensor system have been considered. Using the recommended signal processing solution of PLL followed by a microcomputer, the time constant will be dominated by the signal processing in the case of the pressure and status sensors. The signal processing time constant is related to sensor bandwidth and an appropriate trade-off would be required.

For the temperature sensor, the time constant will be determined by the thermal mass of the sensor itself and this will need to be minimised.

Sensor efficiency

A further major area of development effort will involve the improvement of sensor efficiency so that less light is needed to drive the sensor in oscillation. With the present state of development, it is estimated that the sensors must be arranged in parallel to make maximum use of the available optical power.

If significant improvements in the optical insertion loss can be achieved then mixed parallel and series arrangements become feasible or more sensors could be multiplexed on a given laser. These improvements may be possible by reducing the overall dimensions, and hence the optical path length and loss, and by using reflective coatings on the oscillator paddle.

Transducer packaging

The packaged sensor will have to withstand a variety of environmental conditions. The design, construction and testing of the packaging required to achieve the environmental performance represents a significant development activity.

Smoke detector system

The smoke detector proposed as a result of this work operates on light scattering principles and can therefore be viewed as a separate entity from the other sensors. There are three factors which should be considered in relation to further development of the smoke sensor.

Firstly, there is significant Company background experience in the development of scatter cells and this has already been applied to the construction of devices which can function in a discriminatory way.

Secondly, an experimental programme is required in order to look at variations in smoke types and their scattering properties. This experimental programme would have to include an assessment of window fouling effects since this has been perceived as a major possible drawback to the system. The programme would therefore be a precursor to the full development of a smoke detection system.

The third factor which should be considered is that there is no currently available smoke detector which meets USN needs. The incidence of fire and its consequences are such that further work in this area is of obvious importance.

In conclusion, the different aspects of the proposed fibre optic sensor system have been considered in detail. The conceptual design and basis of operation of the main system elements have been analysed and the key aspects which will need attention in further development have been highlighted.

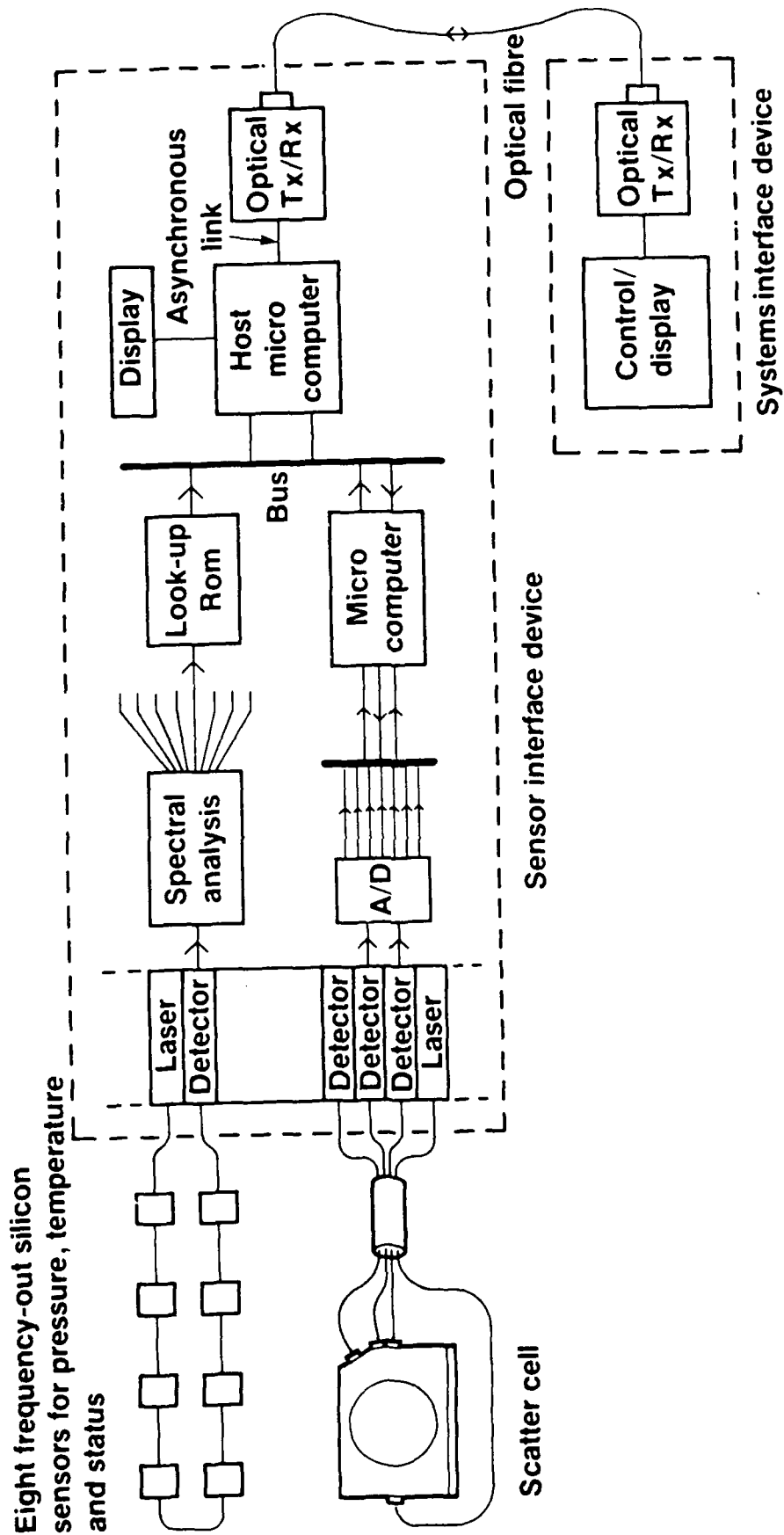


Figure 1. Schematic diagram: Frequency-out silicon sensor and smoke detector system

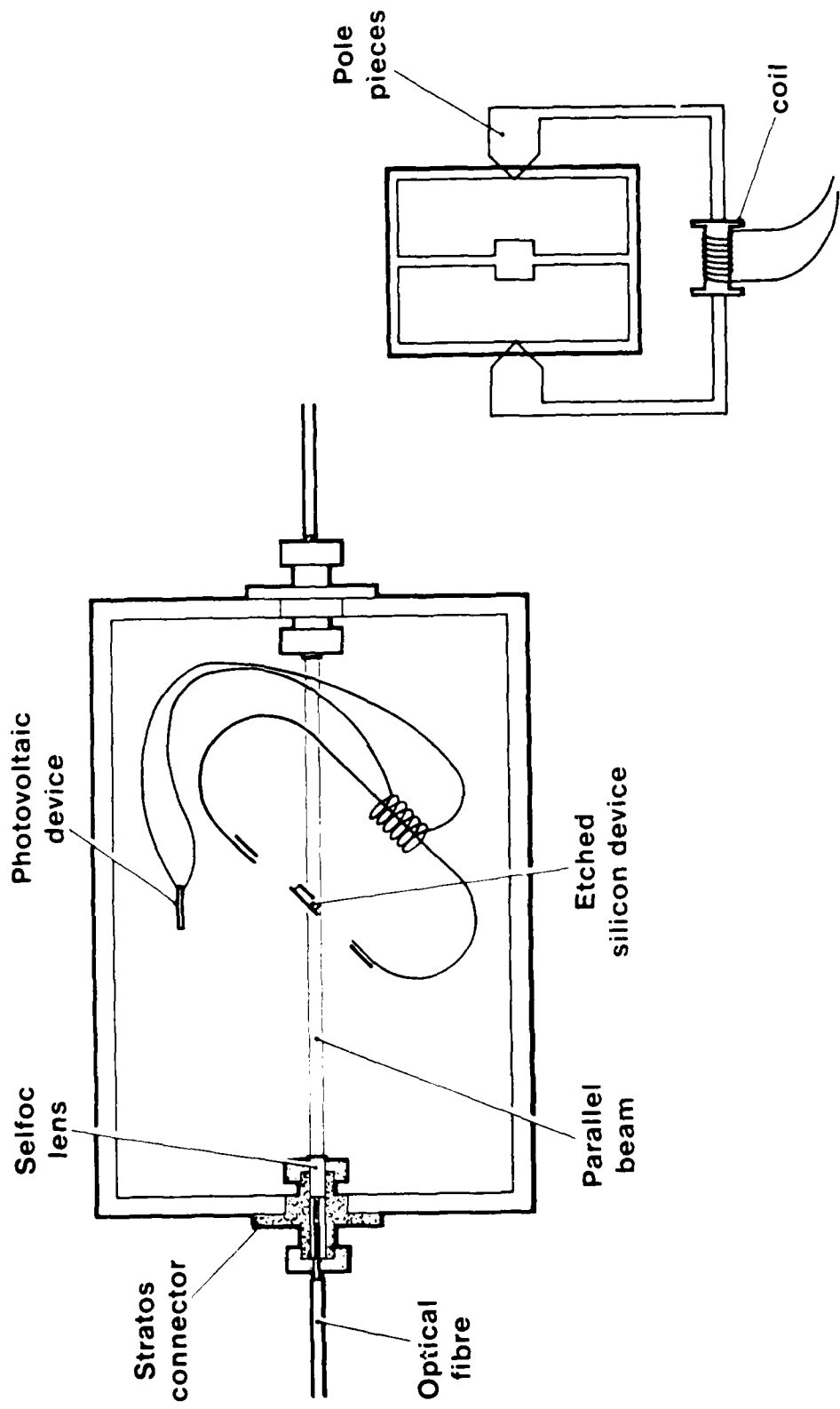


Figure 2. Resonant sensor schematic diagram

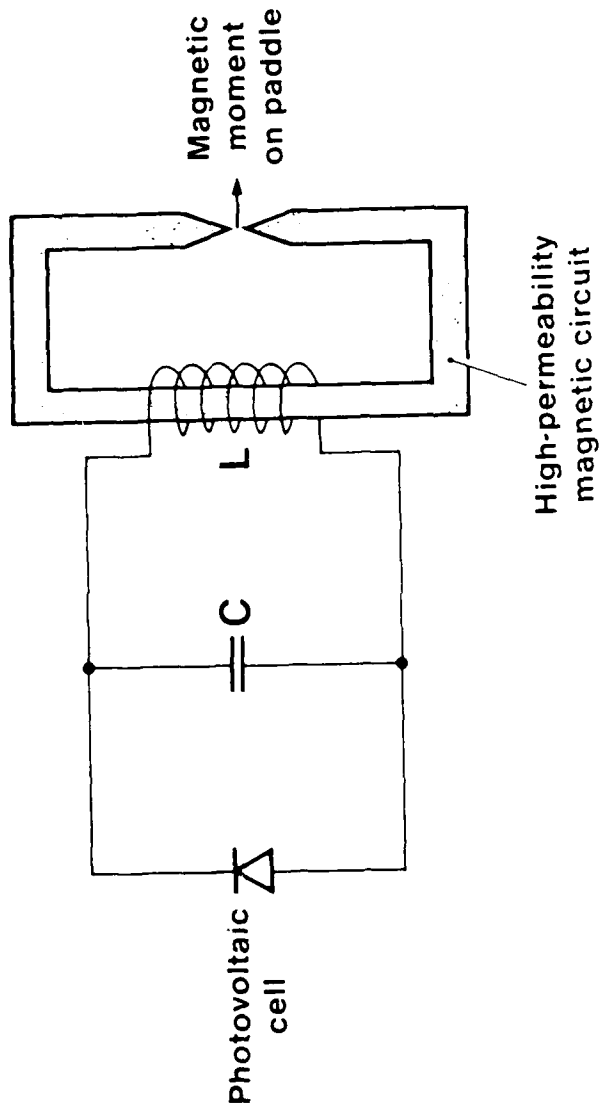


Figure 3. Equivalent circuit of magnetically actuated self-resonant device

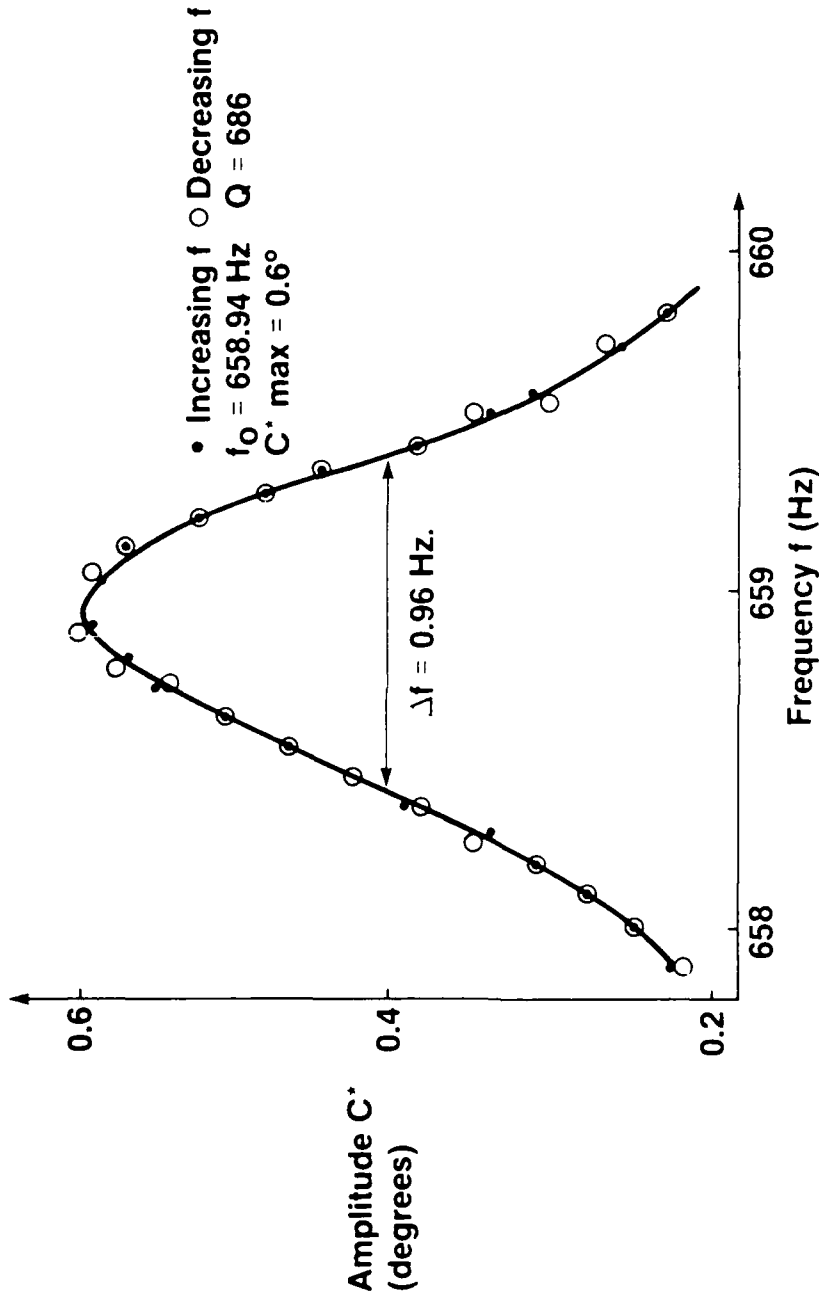


Figure 4. Hysteresis effects due to amplitude: Small amplitude case (Peak amplitude 0.6°) Graph of the measured oscillation amplitude (C^*) as a function of drive frequency for a silicon paddle oscillator. C^* measured for either increasing or decreasing frequency shows a similar response. (Compare with Fig. 5)

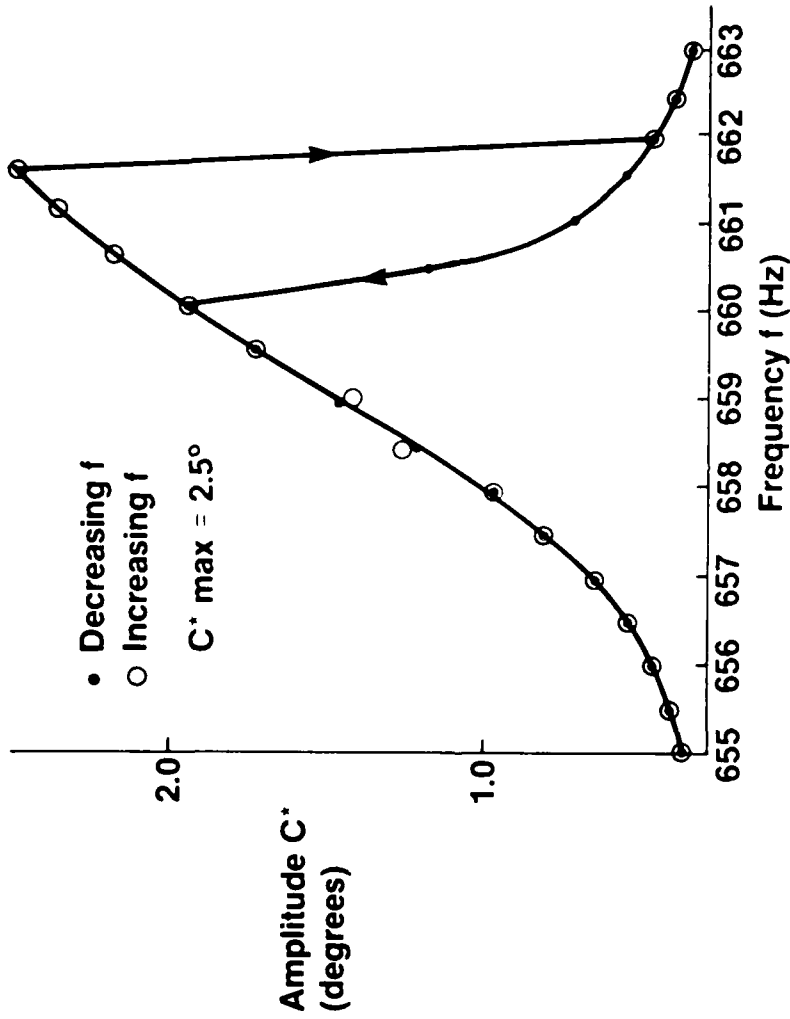


Figure 5. Hysteresis effects due to amplitude: Large amplitude case. (Peak amplitude 2.5°)
Graph of the measured oscillation amplitude (C*) as a function of drive frequency
for a silicon paddle oscillator. C* measured for increasing and decreasing
frequency shows a different response indicating the presence of stress stiffening.
(Compare with Fig. 4)

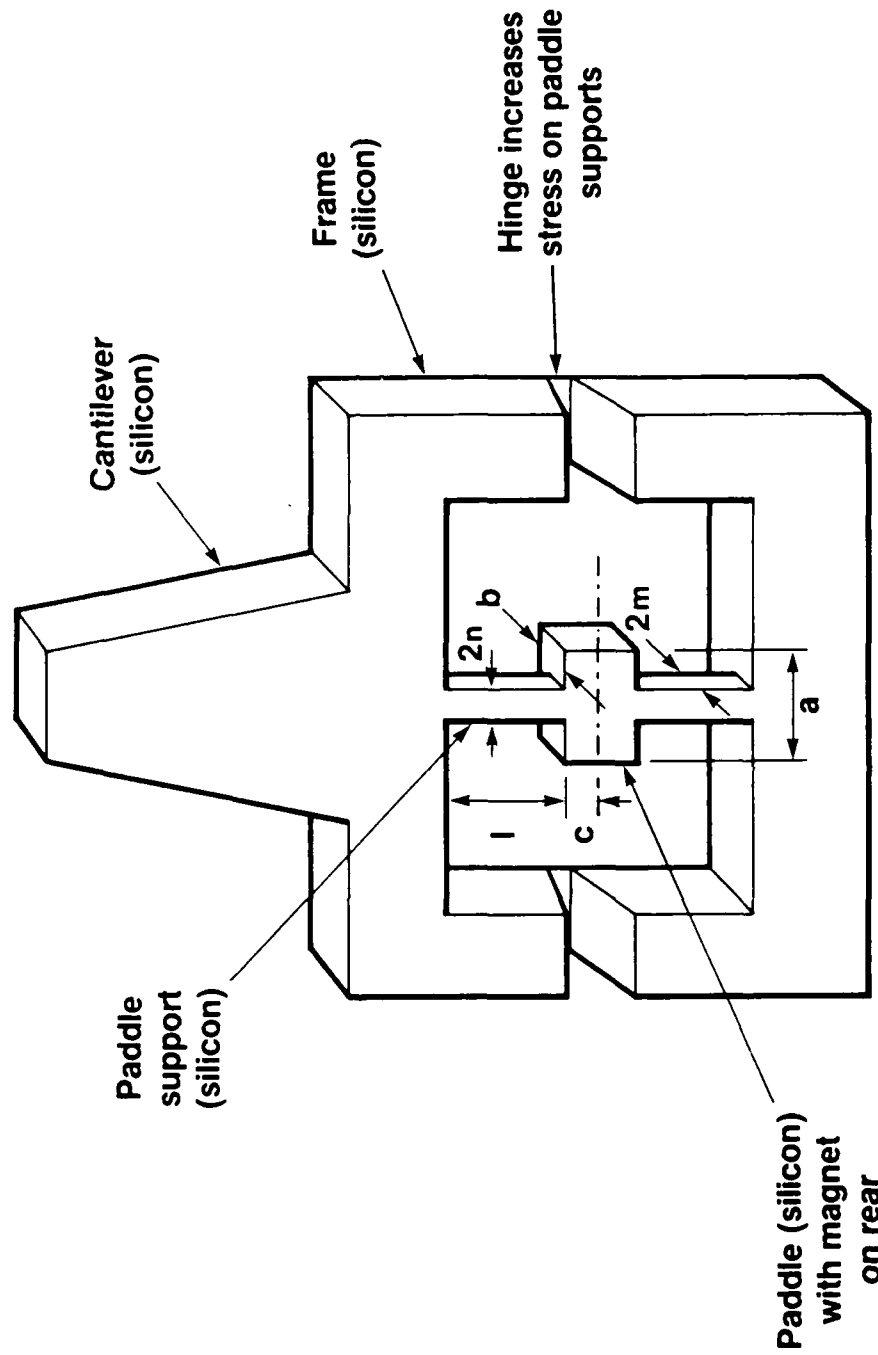


Figure 6. Silicon oscillator

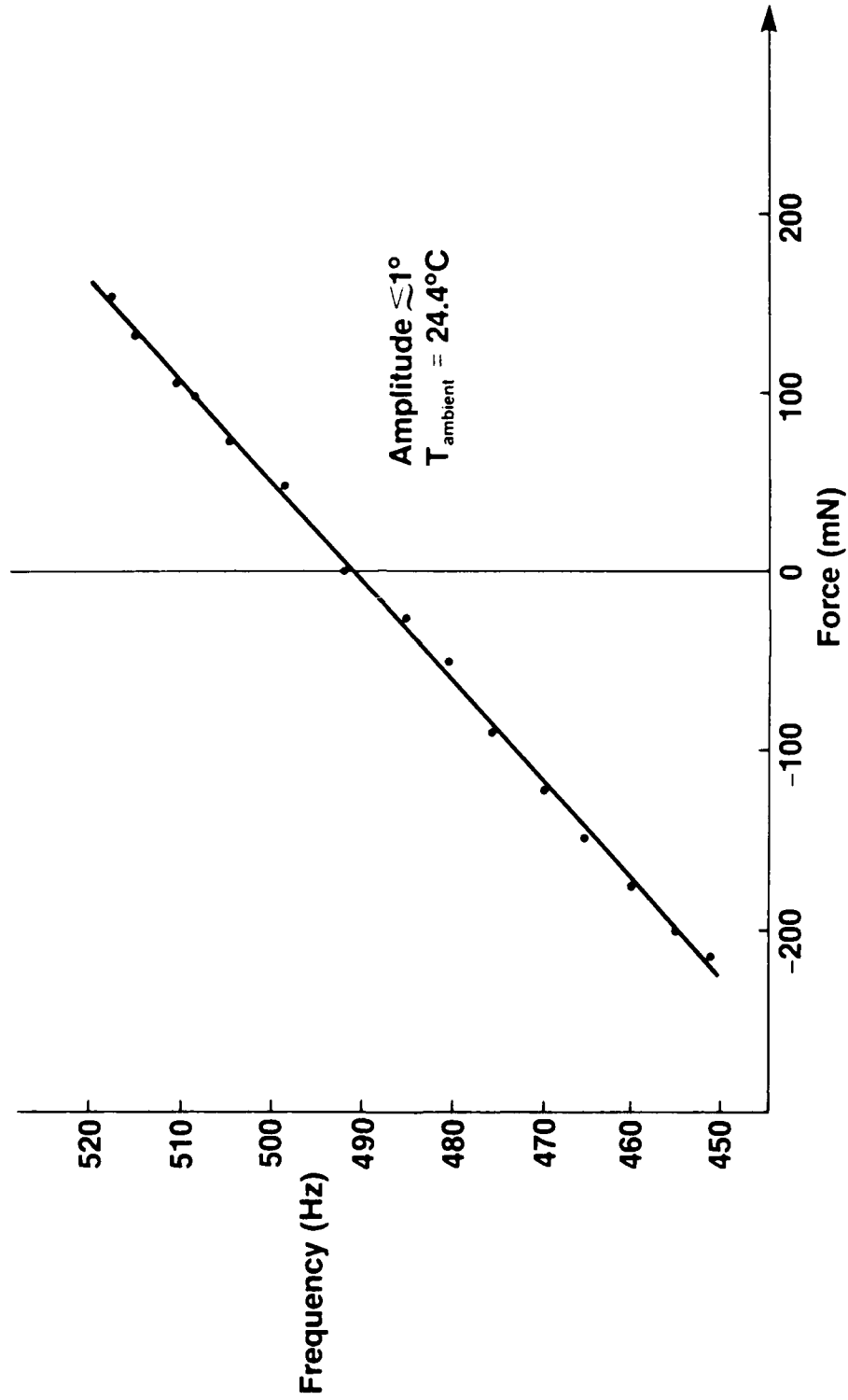


Figure 7. Variation in the resonant frequency of the silicon sensor with the force applied to the cantilever

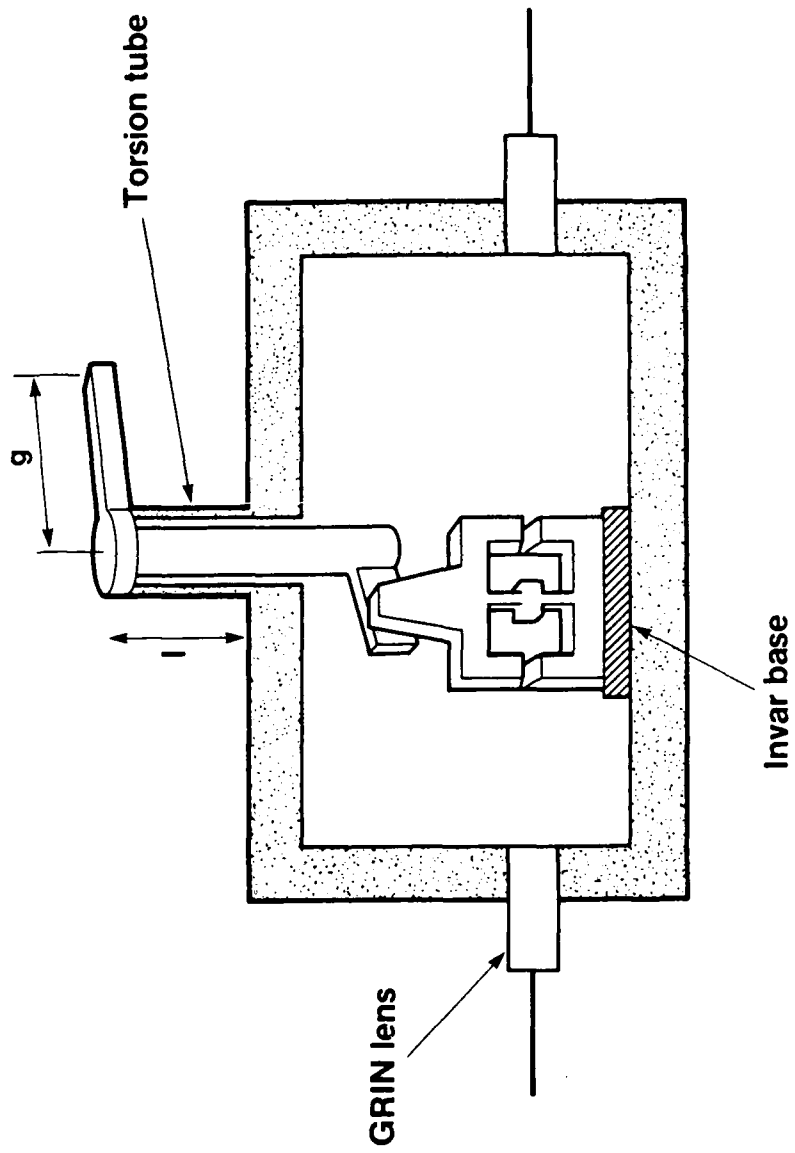


Figure 8. Status, pressure and temperature transduction mechanism

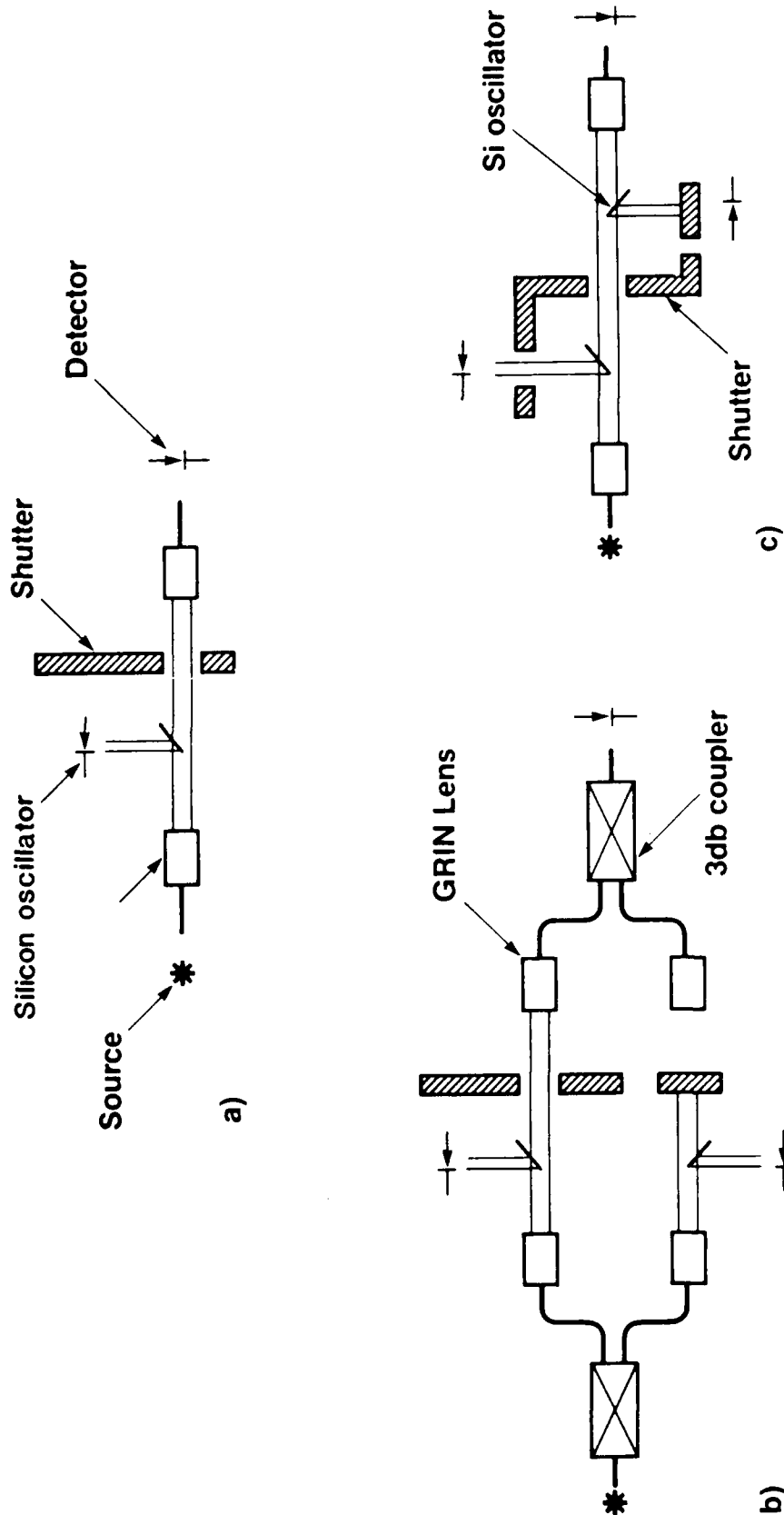


Figure 9. Possible status sensor configurations

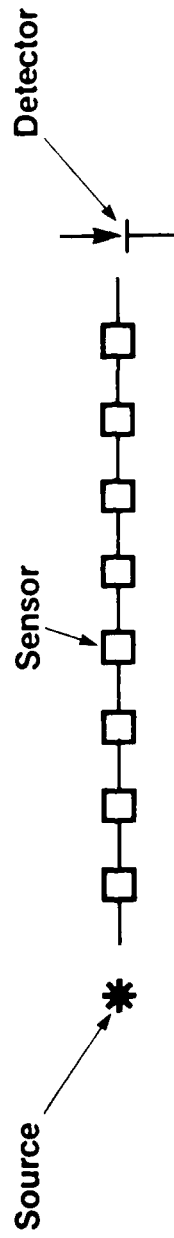


Figure 10. Frequency-out silicon sensor multiplexing, series arrangements

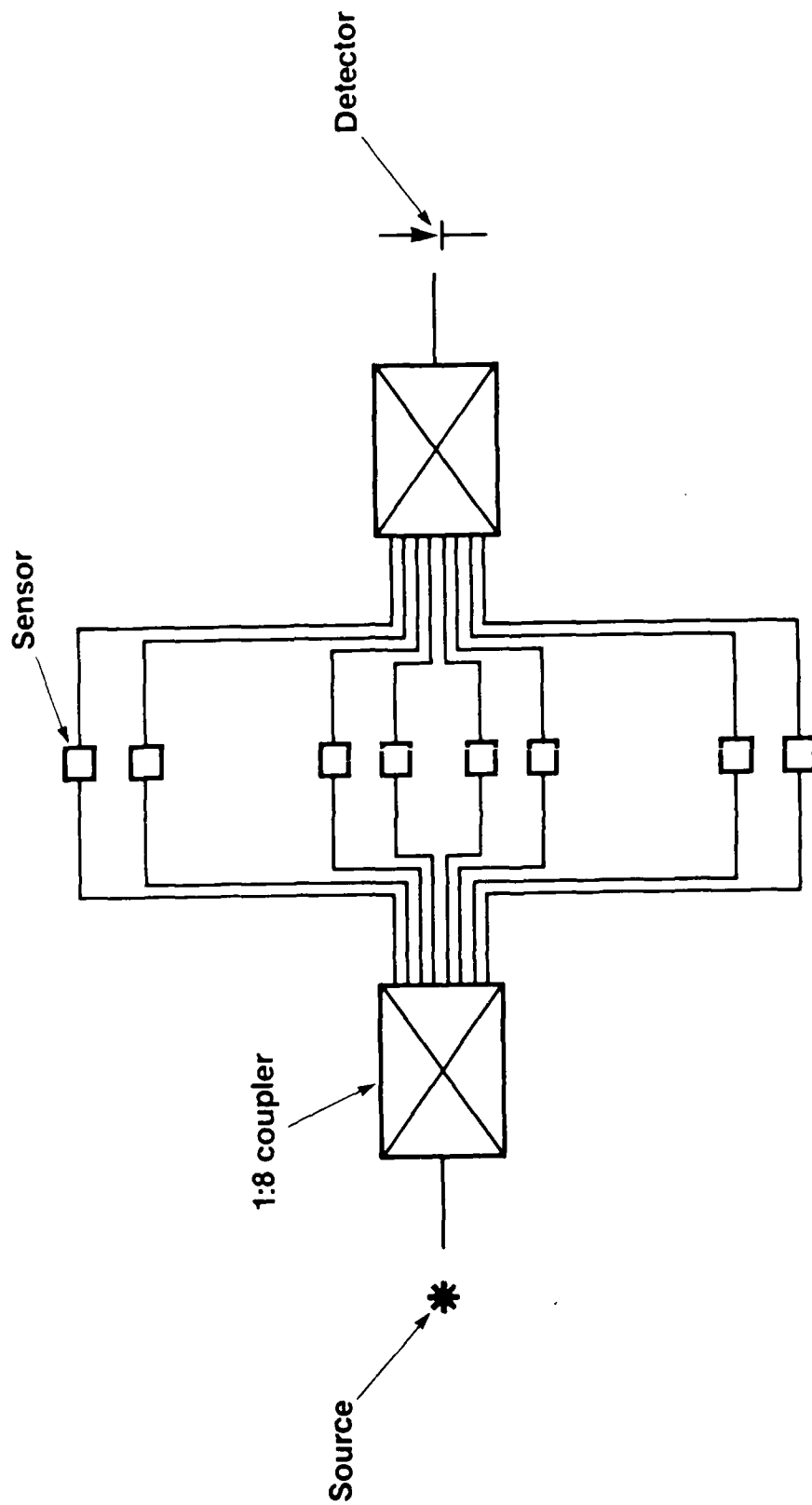


Figure 11. Frequency-out silicon sensor multiplexing, parallel arrangement

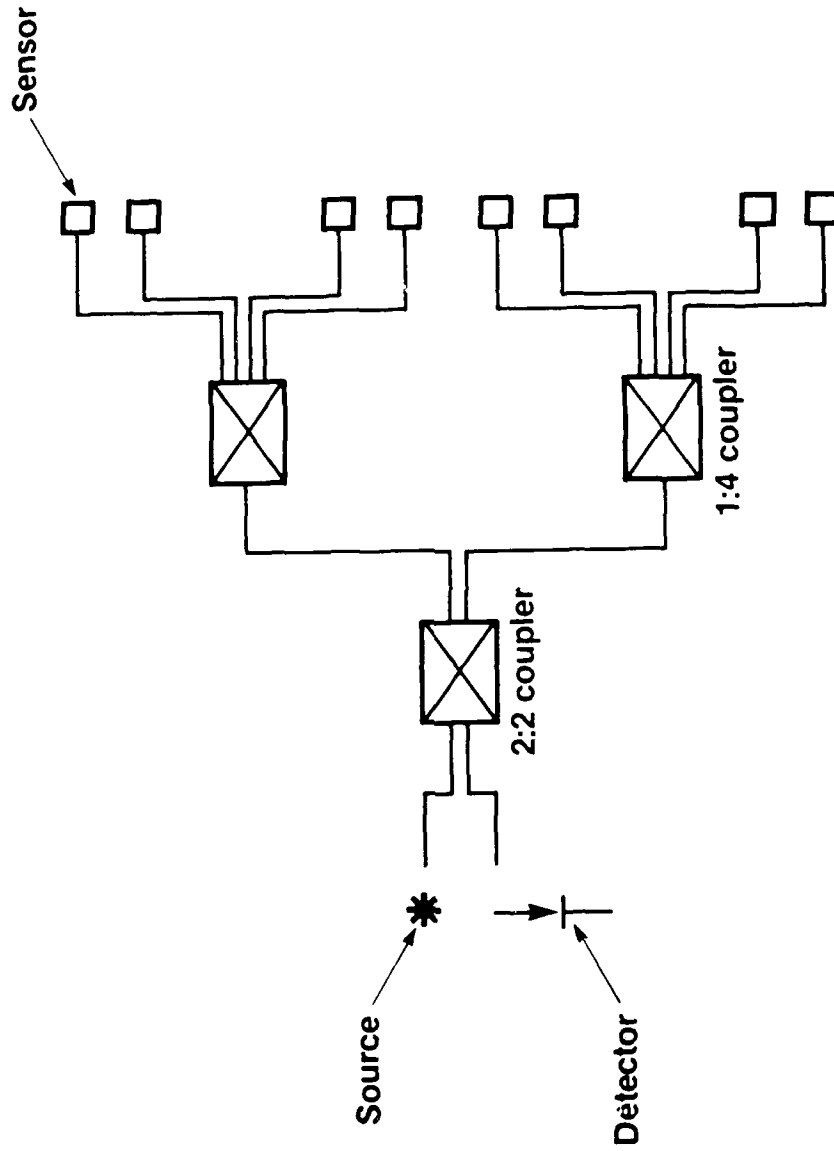


Figure 12. Frequency-out silicon sensor multiplexing, parallel reflective arrangement

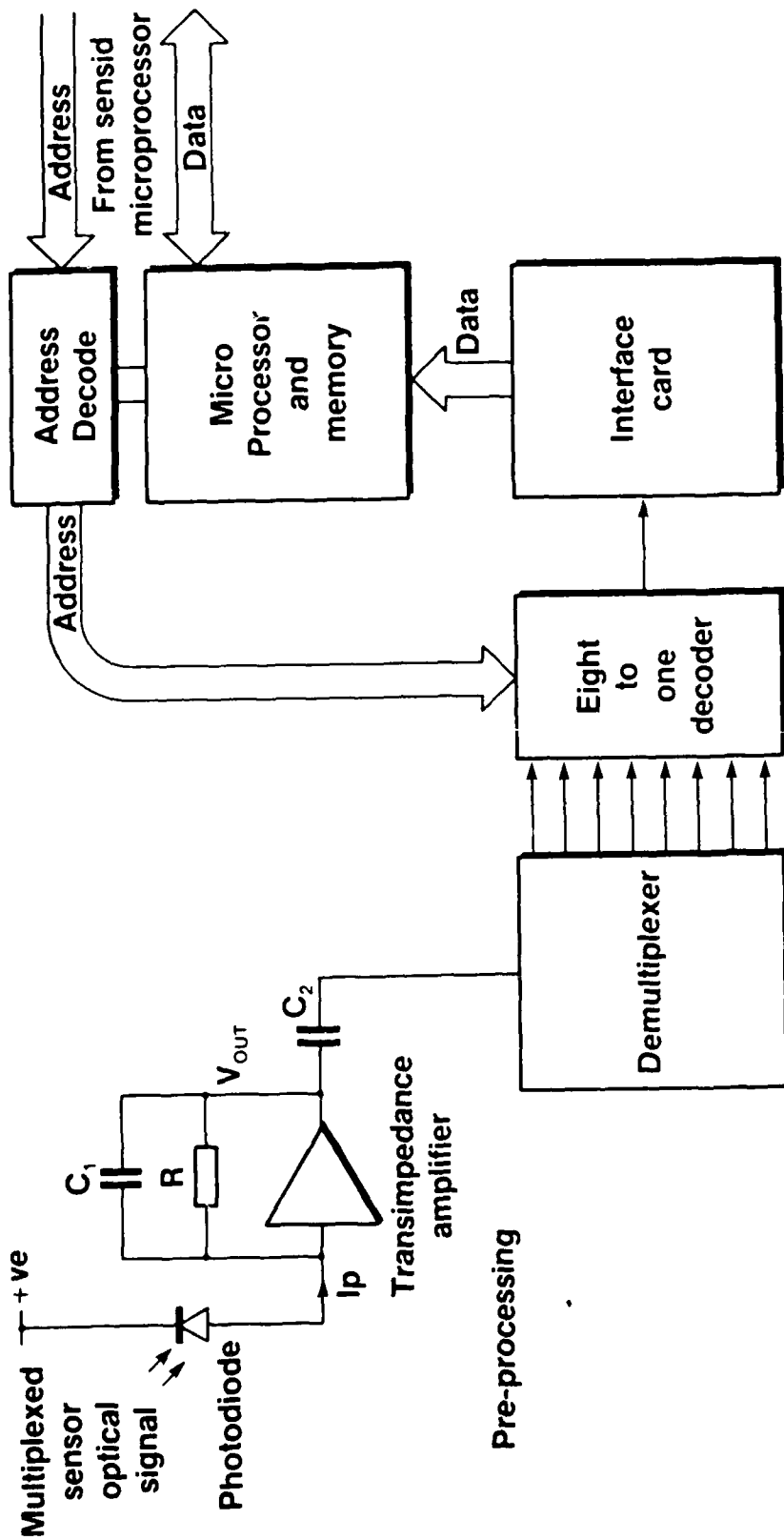


Figure 13. Sensor processing schematic

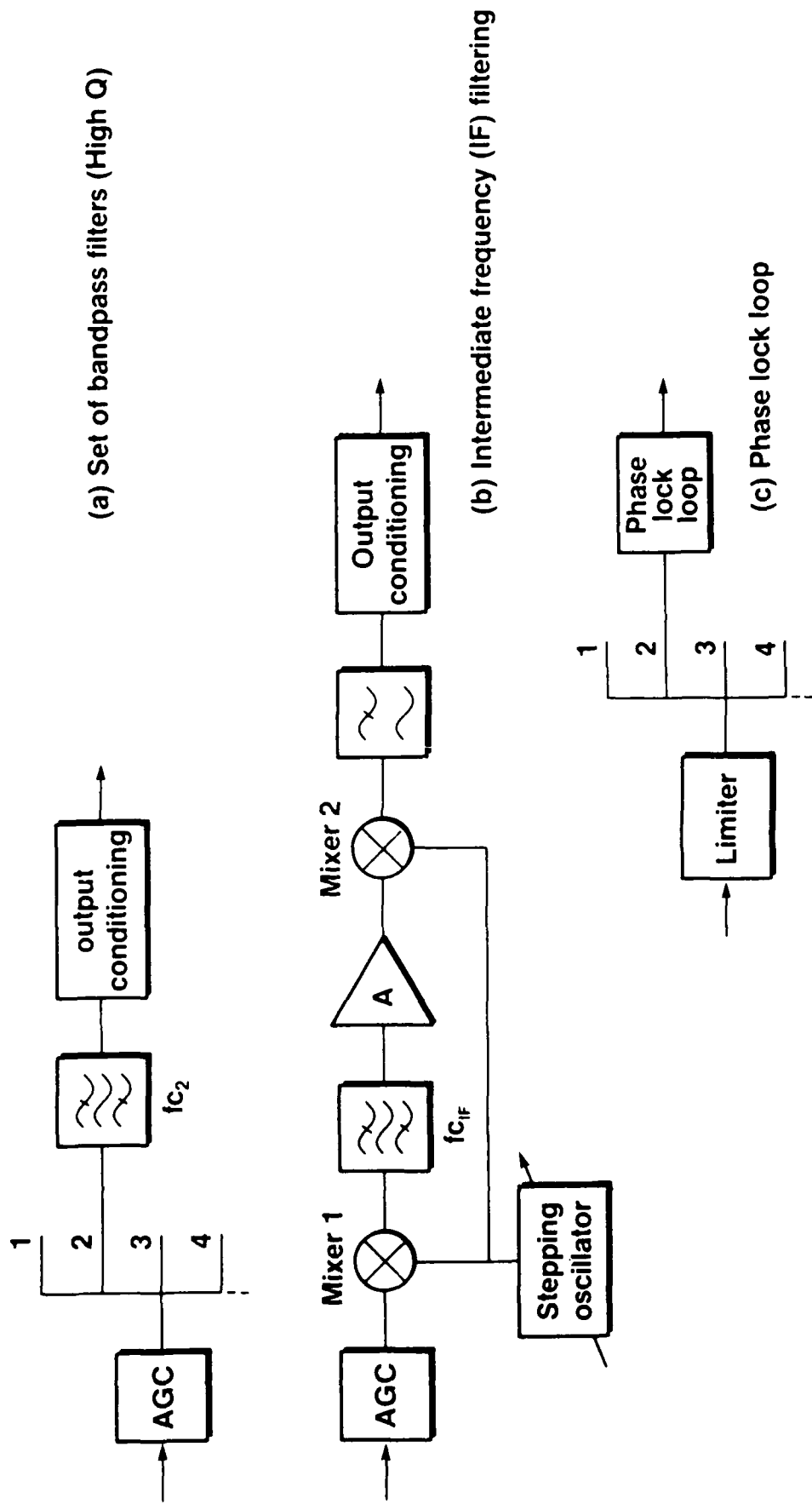


Figure 14. Analogue demultiplexing: alternative solutions

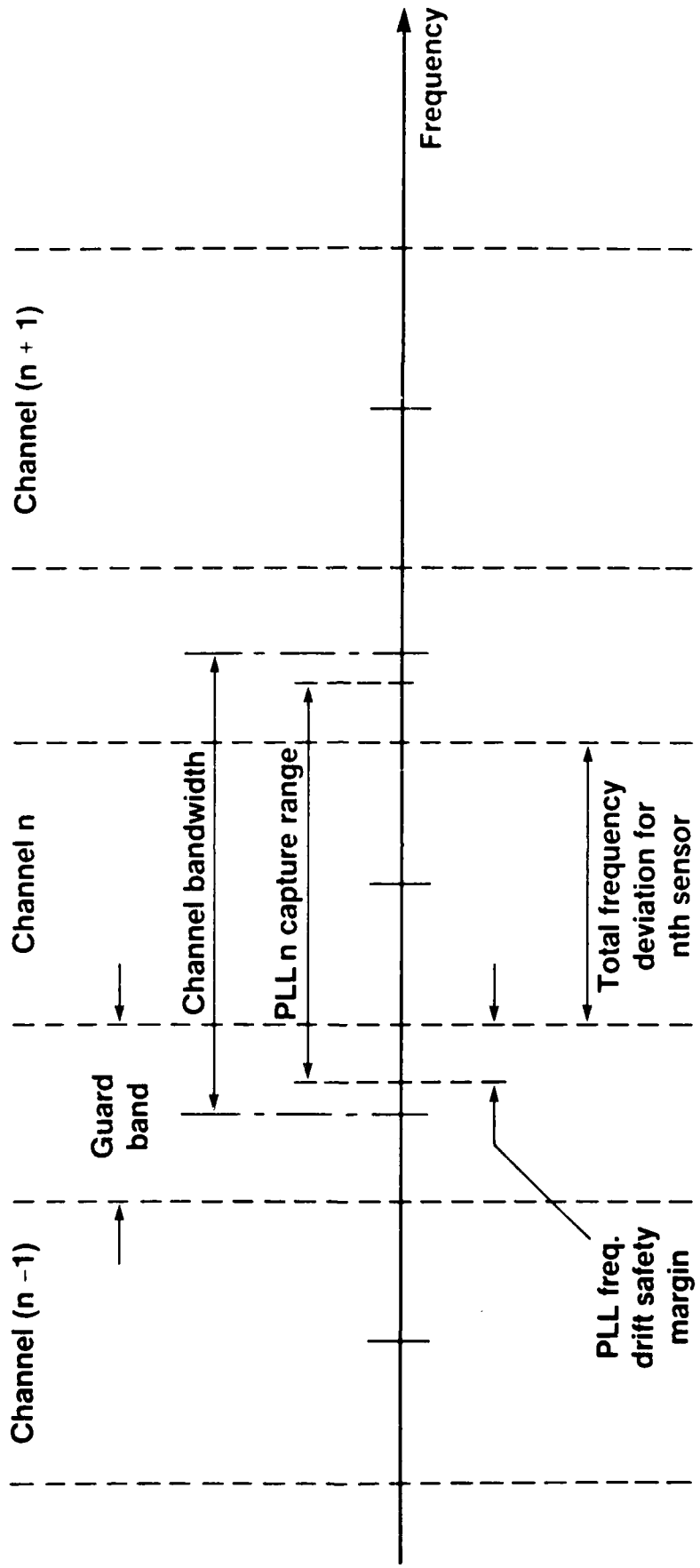


Figure 15. Channel distribution for multiplexed sensors, diagram showing design criteria for phase lock loop capture bandwidth

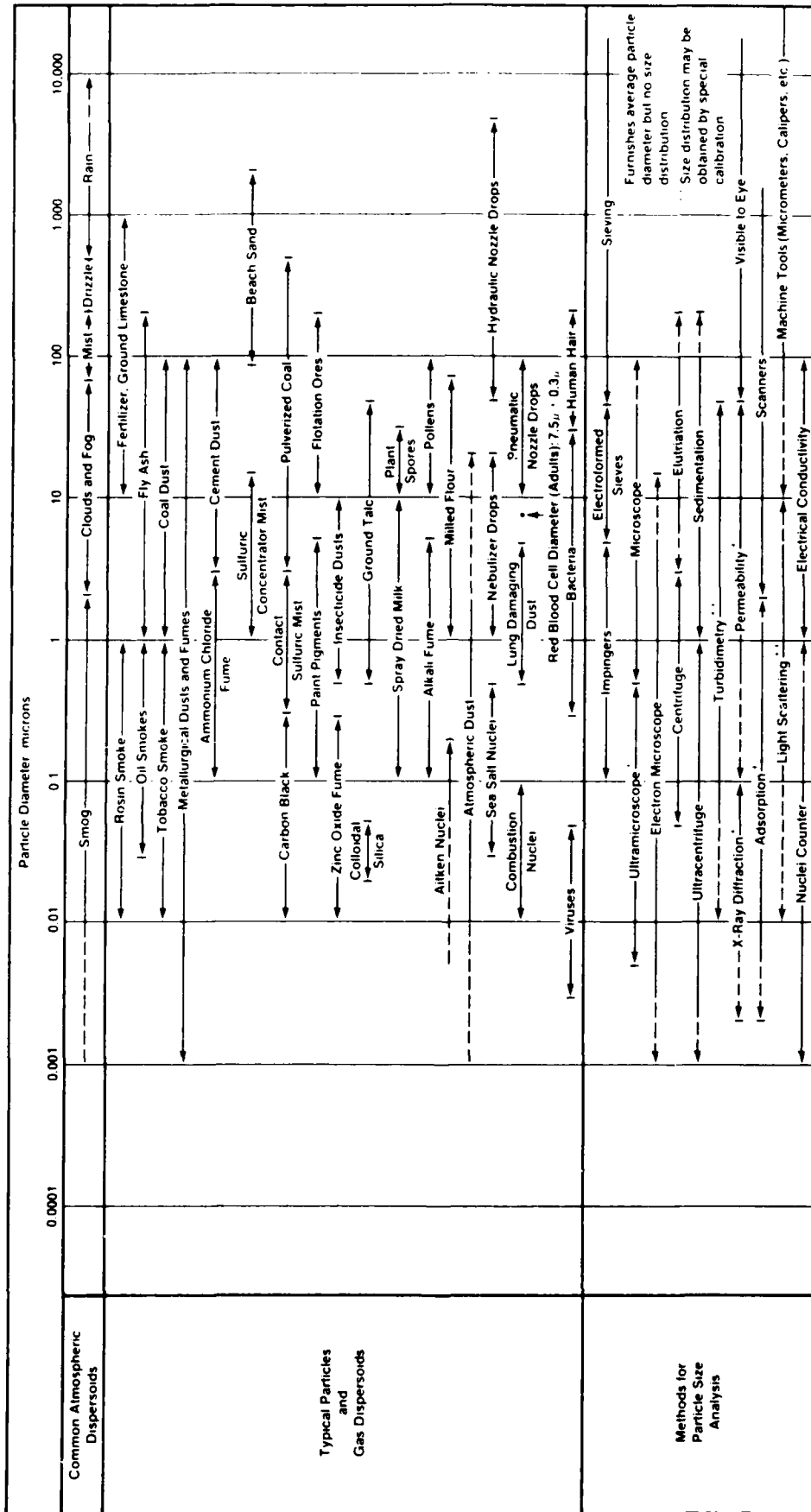


Figure 16. Characteristics of particles and particle dispersoids

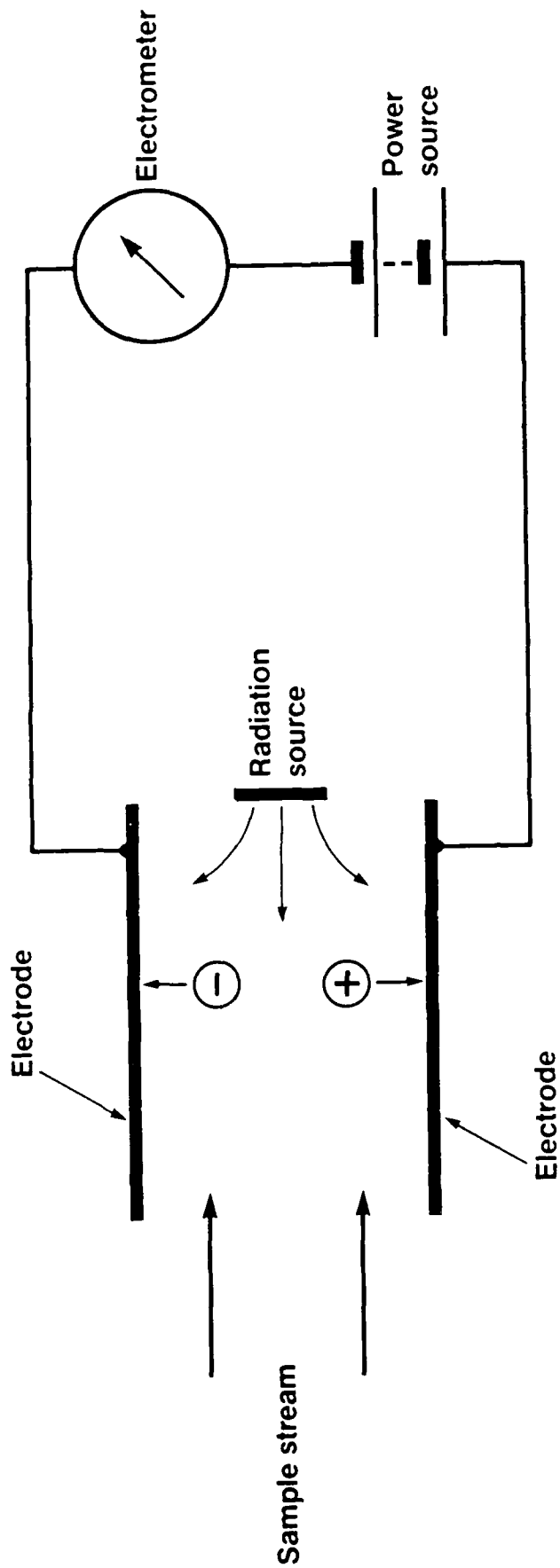


Figure 17. Schematic of simplified ionisation type smoke detector

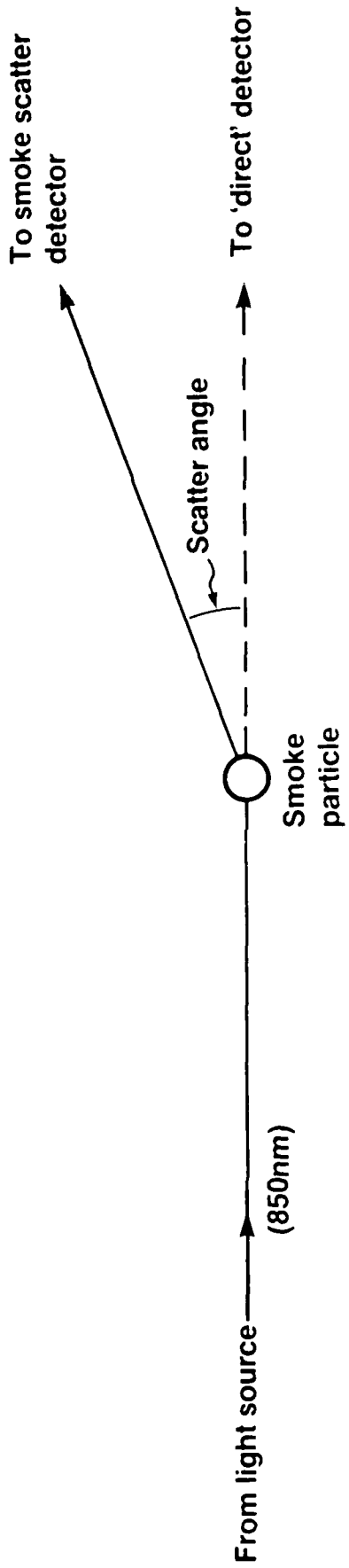


Figure 18. Schematic of light scatter smoke detector

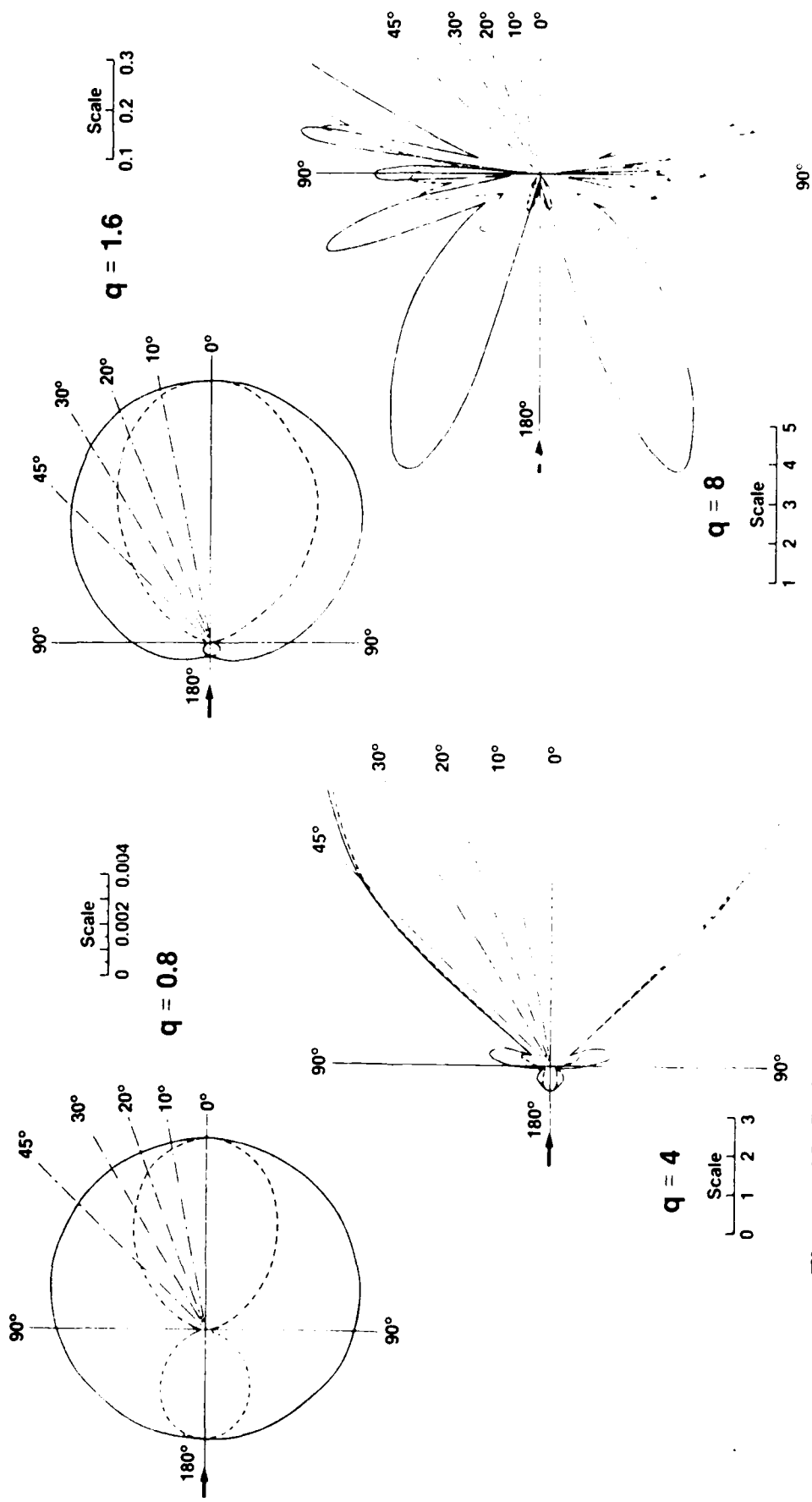


Figure 19. Polar diagrams for the scattering of linearly polarised light by a dielectric sphere of refractive index 1.25

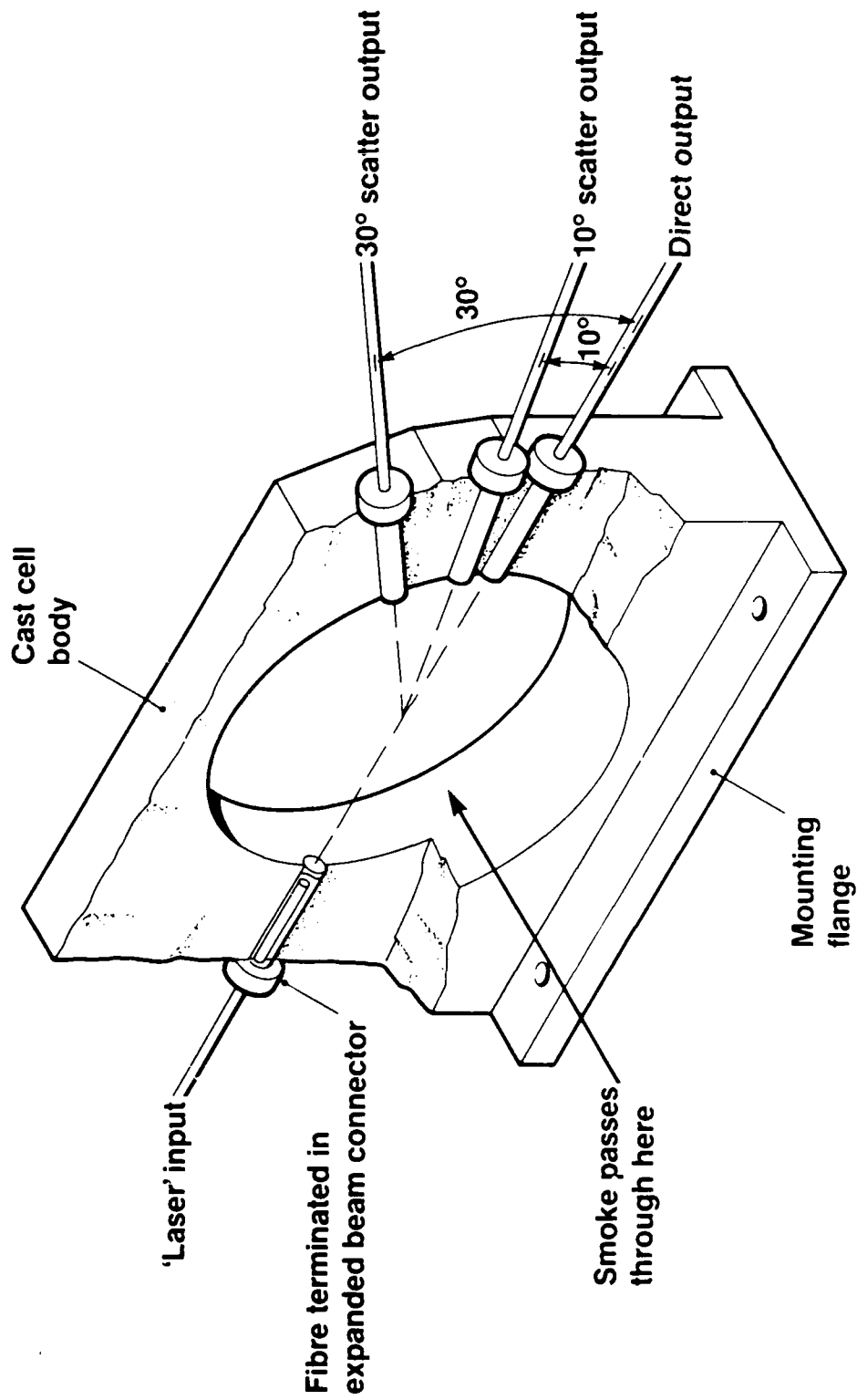


Figure 20. Simple scatter cell schematic

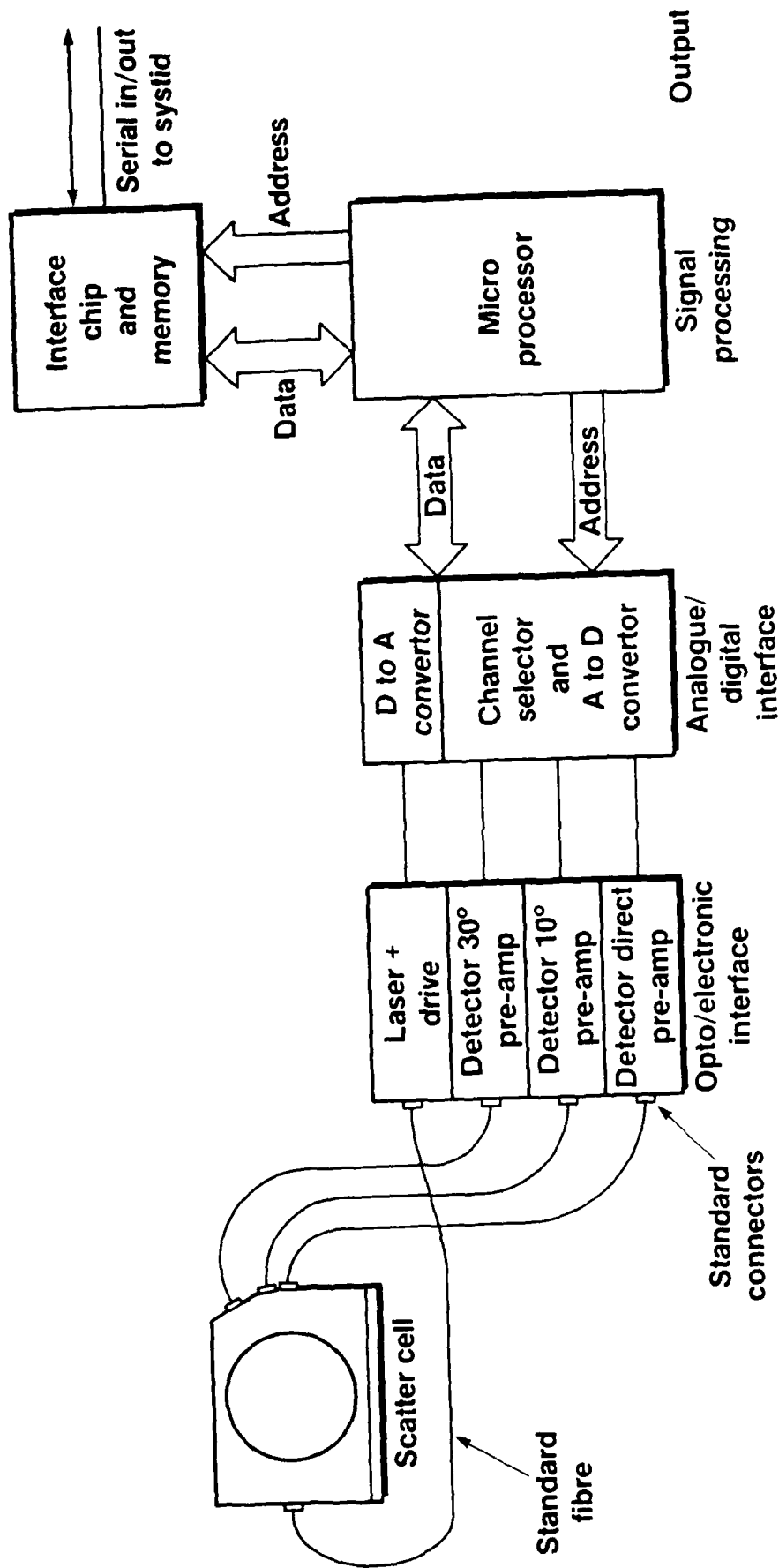


Figure 21. Smoke detector system schematic

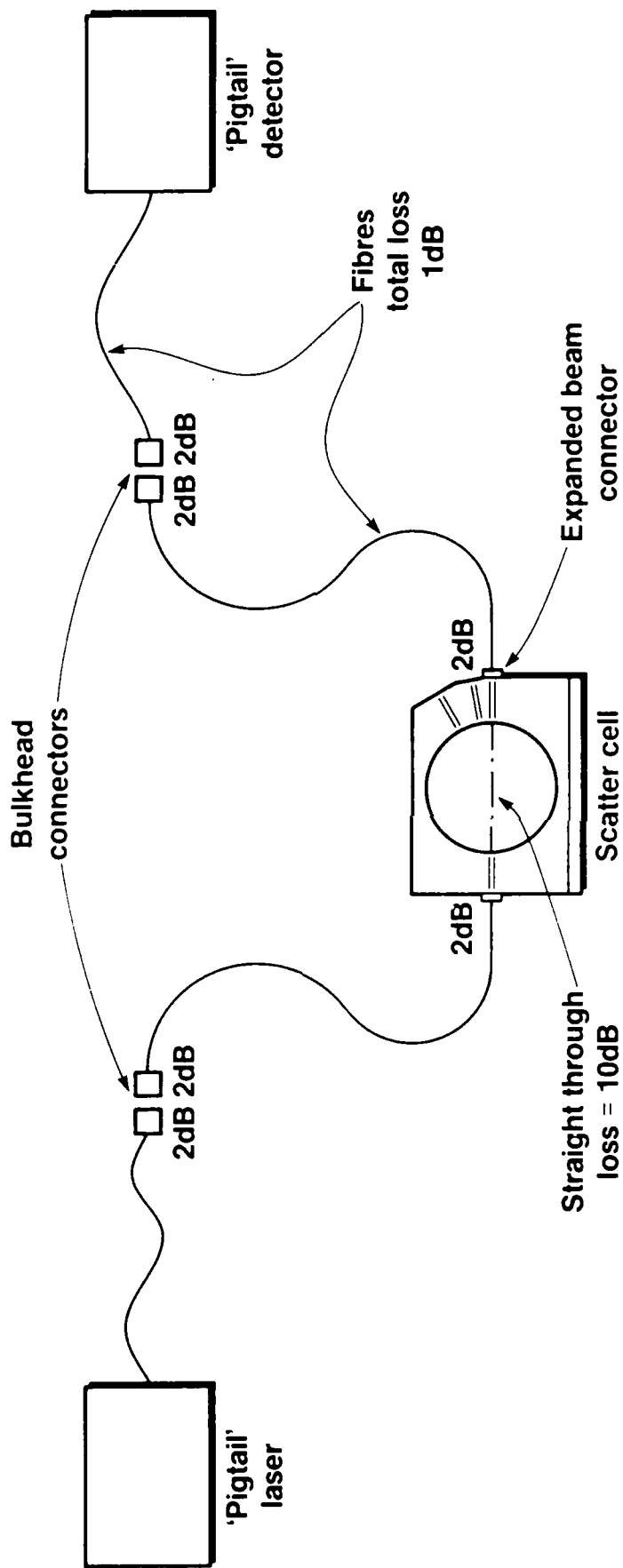


Figure 22. Optical losses in the smoke detector system

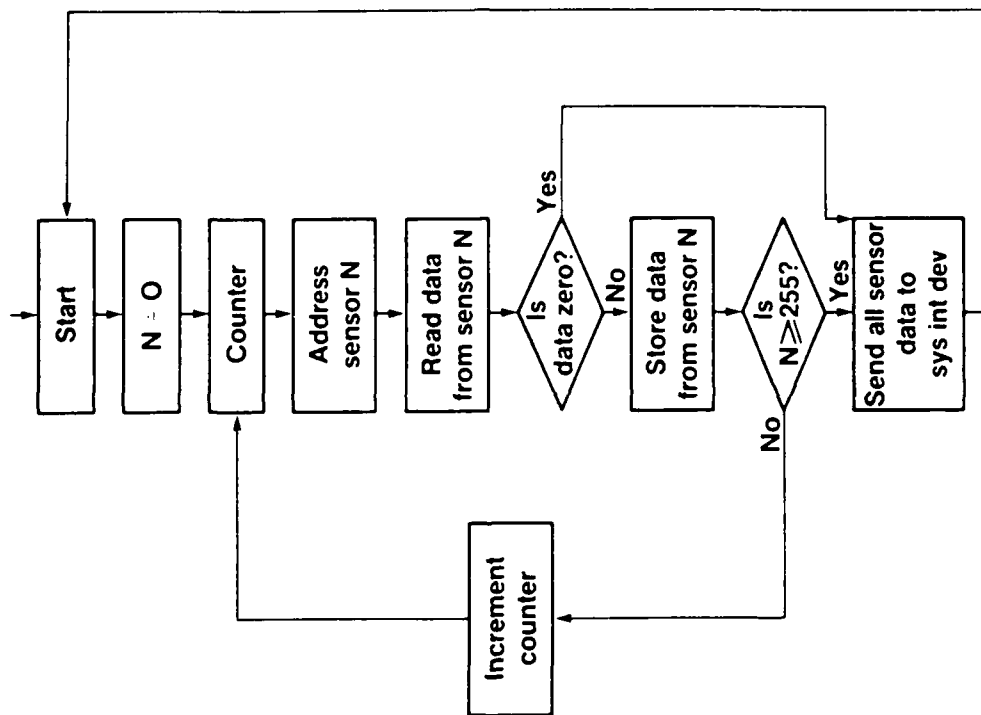


Figure 23. Sensor interface device flowchart

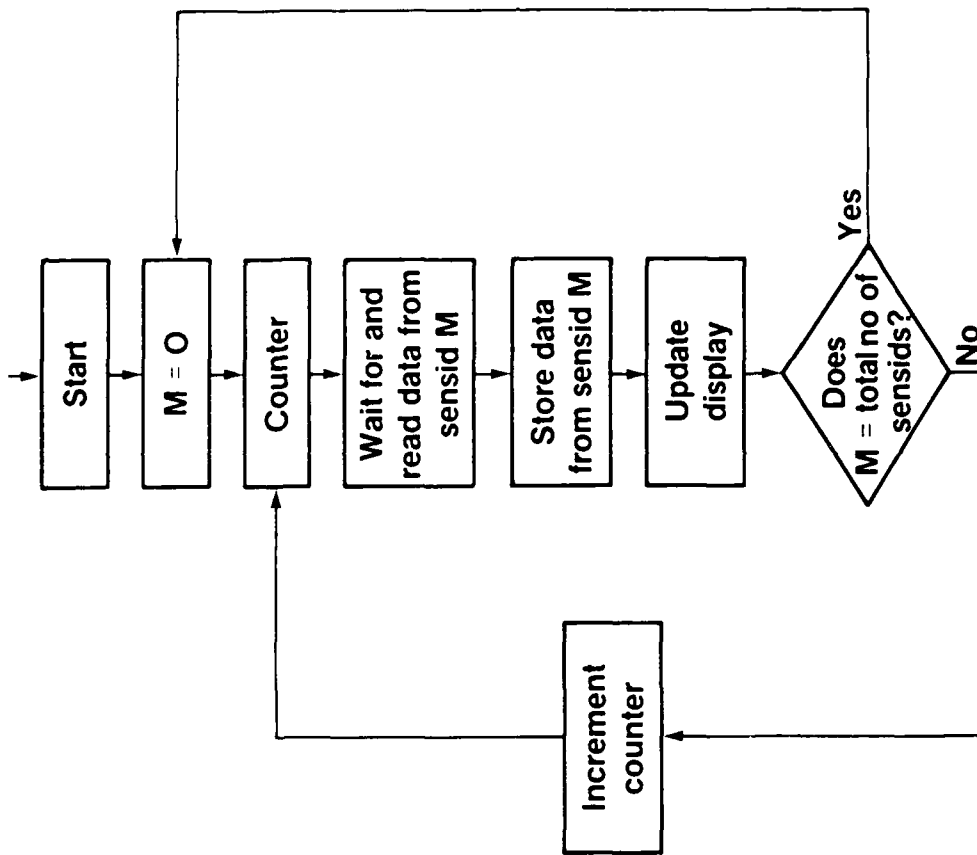


Figure 24. System interface device flowchart

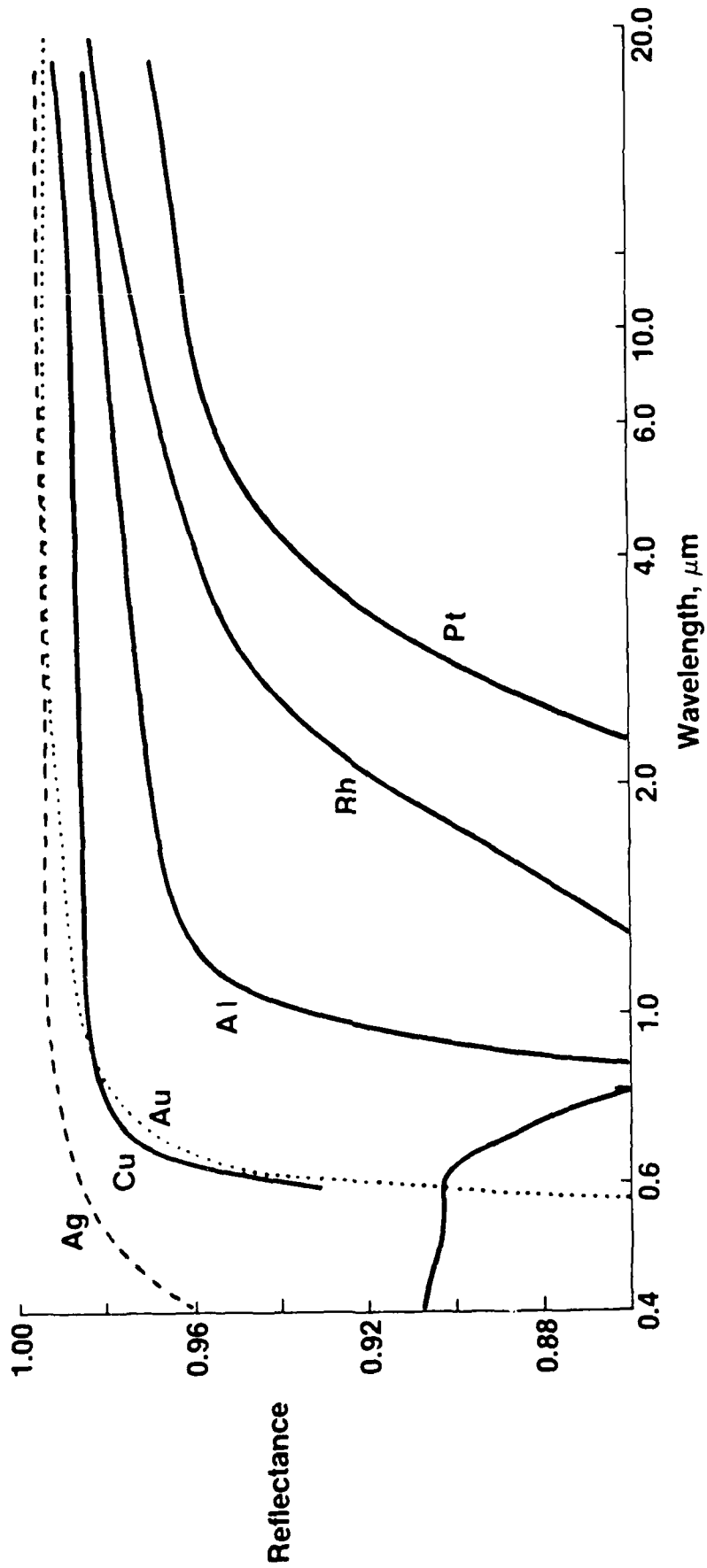


Figure B-1. Visible and infrared reflectance of certain metals

REFERENCES

1. Proposal for the development of a fibre optic sensor system for the United States Navy, STC Defence Systems, Greenwich, England, June 1987.
2. Chesley, V., Code 1232. VC, Contracting Officer, Solicitation number N00014-86-R-VC21, Naval Research Laboratory, Washington, D.C., 19 May 1986.
3. Burrage, M.E., Minutes of meeting held at STL, Harlow, England, 8 June 1987.
4. Williams, F. W., and Carhart, H.W., Consolidated Damage Control System, NRL Memorandum Report 5045, Naval Research Laboratory, Washington, D.C., 8 April 1983.
5. Dimmer, P.R., "Fire-fighting and damage control in surface warships. Recent developments", Transactions of the Institute of Marine Engineers, Section C, Vol. 98 paper C1/6.
6. Akhurst, R., "Sub-division in surface warships", Transaction of the Institute of Marine Engineers, Section c, Vol. 98, paper C1/3.
7. Clements, D.J., and Kneebone, G.P., "Integrated damage surveillance and control in surface warships", Transactions of the Institute of Marine Engineers, Section C. Vol. 98, paper C1/11.
8. Brown, D. K., "Ships that survive", Maritime Defence, July 1985, 234.
9. "Survivability in the nuclear age", Maritime Defence, July 1985, 233.
10. Willrodt, G., "NBC protection in modern naval ship design", Maritime Defence, July 1985, 237.
11. "Type 23 frigate", Navy International, April 1986, 201.
12. "Naval firefighting - lessons learned from the Falklands", Safety at Sea, August 1986.
13. Dimmer, P.R., "Fire-fighting in warships: Lessons from the Falklands conflict", Marine Engineers Review, January 1986, 6.
14. Giallorenzi, T.G., Bucaro, J.A., Dandridge, A., Sigel, G.H., Cole, J.H., Rashleigh, S.C. and Priest, R. G., "Optical Fibre Sensor Technology", IEEE Journal of Quantum Electronics, Vol. QE 18, No. 4, April 1982, pp 626 - 665.

15. Pilt, G.D., Extance, P., Neat R.C., Batchelder, D.N., Jones, R.E., Barnett, J.A. and Pratt, R.K., "Optical-fibre sensors", IEE Proceedings, Vol.132, Pt.J, No.4, August 1985, pp 214-248.
16. Greenwood, J.C., "Ethylene diamine-catechol-water mixture shows preferential etching of p-n junction", Journal of the Electrochemical Society, 1969, Vol. 116, pp 1326-1327.
17. Petersen, K.E., "Silicon as a mechanical material", Proceedings of the IEEE, 1982, Vol.70, pp 420-455.
18. Angell, J.B., Terry, S.C. and Barth, P.W., "Silicon Micromechanical devices", Scientific American, April 1983, pp 36-47.
19. Greenwood, J.C., "Etched silicon vibrating sensor", Journal of Scientific Instrumentation, 1984, Vol. 17, pp 650-652.
20. Adolfsson, M. and Brogardh, T., "Fiber Optical devices for measuring physical phenomena", US Patent, 4 345 482, 1982.
21. Greenwood, J.C, "Transducer", UK Patent Appln. No.121 953A, 1982.
22. Ovren, C., Adolfsson, M. and Kole, B., "Fibre Optic Systems for temperature and vibration measurements in industrial applications", Proceedings of the International Conference on Optical Techniques in Process Control, 14-16 June 1983, Den Haag, pp. 67-81.
23. Snel, D. and Pitt, G.D., "Oil content monitoring (practical considerations)", Proceedings of the International Conference on Optical Techniques in Process Control, 14 - 16 June, 1983, Den Hagg, pp. 27-41.
24. Extance, P. and Pitt, G.D., "Intelligent turbidity monitoring", Proceedings of the International Conference on Optical Techniques in Process Control, 14 - 16 June, 1983, Den Haag, pp 43 - 54.
25. Palais, J.C., "Fiber Coupling using graded-index lenses", Applied Optics, Vol. 19, 1980, p. 2011.
26. Roark, R.J. and Young, W.C., Formulas for stress and strain, McGraw Hill, 1976, 5th Edition, section 9.4, p 316 ff.
27. Reference 26, p 96.
28. Benham, P.P. and Warnock, F.V., Mechanics of solids and structures, Pitman, 1976, section 1.15, p 24 ff.

29. From manufacturer's data, Argon Manufacturing Co. Ltd., 26 Breakfield, Coulsden, Surrey, CR3 2HS, England.
30. Reference 26, Table 20, p.292.
31. From manufacturer's data, Hydroflex, Unit KLI, Kingsville Road, Kingsditch Trading Estate, Cheltenham, Glos., GL51 9PR, England.
32. Sakai, I., "Frequency-division multiplexing of optical fibre sensors using a frequency modulated source", Optical and Quantum Electronics, 1986, Vol. 18, p.279.
33. Moschytz, G.S., "Miniaturised RC filters using Phase Locked Loop", Bell System Tehnical Journal, May 1965.
34. Linden, G., "Test methods for fire detection equipment at the laboratory of the Verband der Sachversicherer (Cologne)", Proceedings 6th Symposium of Department of the Environment and Fire Officers Committee, London, March 1972.
35. Mulholland, G.W. and Liu, B.Y.H., "Response of Smoke Detectors to Monodisperse Aerosols", Journal of Research of the National Bureau of Standards, Vol. 85, No. 3, June 1980.
36. Lapple, C.E., "The little things in Life", Stamford Research Institute Journal, 1961, Vol. 5/94 3rd quarter, pp 95 - 102.
37. Waters, G.E., "Fire detection in large enclosed spaces", Proceedings 6th Symposium of Department of the Environment and Fire Officers Committee, London, March 1972.
38. Green, H.L., and Lane, W.R., Particulate clouds, E. & F.N. Spon Ltd., 2nd Edn., 1964, Chapter 4, "Optical Properties".
39. Born, M. and Wolf, E., Principles of Optics - Electromagnetic theory of propagation interference and diffraction of light, Pergamon Press, 6th Edn. 1985.
40. Gregorig, I., Measurement of light levels and attenuations in the Oilcon Optical System, Report No. IR/442/1978/760, STC Technology, Harlow, England, 1978.
41. Kip, A.F., Fundamentals of Electricity and Magnetism, McGraw Hill, 2nd Edn. 1969, Section 11.7 p 403 ff.
42. Kreysig, E., Advanced Engineering Materials, J. Wiley, 4th Edn. 1979, Section 2.13 p 113 ff.
43. Ref.26, Table 36, p 578.

Bibliography

Gardner, F.M., Phase Lock Techniques, John Wiley, 2nd Edn, 1979.

Nash, G., Phase Lock Loop design fundamentals, Application Note 535, Motorola, 1970.

Ludlow, I., Analysis of the optical path in the Oil Content Monitor, Report No. IR/442/1978/722, STC Technology, Harlow, England, 1978.

Charlson, E.J., Horvath, H. and Pueschel, R.F., Atmospheric Environment, Pergamon Press, Vol. 1, 1967, pp 469 - 478.

Grehan, G., Maheu, G. and Gouesbet, G., "Scattering of laser beams by Mie scatter centres: numerical results using a localised approximation", Applied Optics, Oct. 1986, vol. 25, no. 19, pp. 3539 - 3548.

Walter, D.P., Cooper, D.E., Laan, J.E. vd. & Murray, E. R., "Carbon dioxide laser backscatter signatures from laboratory generated dust", Applied Optics, August 1986, Vol. 25, No. 15, pp. 2506 - 2513.

Gomi, H., "Multiple Scattering correction in the measurement of particle size and number by the diffraction method", Applied Optics, Oct. 1986, Vol. 25, No. 19, pp. 3552 - 3557.

Extance, P., Bilge monitor multi-angled detection and cost reduction, Report No. IR/330/1982/1096, STC Technology, Harlow, England, 1982.

Components of automatic fire detection systems, BS 5445, Part 7, British Standards Institute, London.

Smoke Detectors for fire protective signaling systems, UL 268, Underwriters Laboratories Inc., Northbrook, Illinois.

Smoke Detectors for duct application, UL 268A, Underwriters Laboratories Inc. Northbrook, Illinois.

Perkins, H. C., Air Pollution, McGraw Hill.

Appendix A

Derivation of the resonant frequency for a silicon oscillator.

The electric circuit for the silicon sensor is shown in Fig. 3 and consists of an inductor L with resistor R*, a capacitor C in parallel and a photodiode. The current through the inductor (i') is related to the current produced by the diode (i) by

$$i' = iZ/Z' \quad \dots\dots(A.1)$$

where Z is the impedance of the LC circuit given by (Ref. 41)

$$Z = 1/[j\omega C + 1/(R^* + j\omega L)] \quad \dots\dots(A.2)$$

and Z' is the impedance of the inductor given by

$$Z' = R^* + j\omega L \quad \dots\dots(A.3)$$

It is convenient to write the complex number Z/Z' in terms of its modulus and argument

$$\begin{aligned} |Z/Z'| &= 1/[(1-\omega^2 LC)^2 + \omega^2 C^2 (R^*)^2]^{1/2} \\ -h &= \arg(Z/Z') = \arctan[-\omega CR^*/(1-\omega^2 LC)] \end{aligned} \quad \dots\dots(A.4)$$

Thus, at time s, if

$$i(s) = i^* \cos(\omega s) \quad \dots\dots(A.5)$$

where i* is the peak value of i, then

$$i'(s) = i^* |Z/Z'| \cos(\omega s - h) \quad \dots\dots(A.6)$$

The magnetic flux U(s) produced by the inductor is proportional to i'(s) and hence so is the magnetic field B(s) in which the paddle sits.

The torque t(s) acting on the paddle is given by

$$\begin{aligned} \underline{t}(s) &= \underline{B}(s) \cdot \underline{m} \\ \text{This leads to } t(s) &= |B(s)| |\underline{m}| \end{aligned} \quad \dots\dots(A.7)$$

for $v=90^\circ$, where v is the angle between the B field vectors, ie. small oscillations.

Hence,

- t(s) is proportional to i'(s) - no phase change or pi phase change if \underline{m} reversed.
- no frequency dependence in proportionality constant.

For a torsional simple harmonic oscillator driven by a torque
 $t(s) = t' \cos (Ws),$

$$u(s) = C \cos (Ws - h^*) \quad \dots (A.8)$$

where, according to (Ref. 42)

$$C^* = t' / (J^2 [(W^*)^2 - W^2]^2 + W^2 Y^2)^{1/2} \quad \dots (A.9)$$

$$\tan (h^*) = WY / J [(W^*)^2 - W^2] \quad \dots (A.10)$$

$$W^* = (GK / JI)^{1/2} \quad \dots (A.11)$$

G = shear modulus

K = torsional stiffness constant (Appendix C)

J = mass moment of inertia of lumped end mass (half the paddle)

Y = velocity damping constant

Hence

$$u(s) \text{ is proportional to } C^* / t' |Z/Z'| \cos(Ws - h - h^*) \quad \dots (A.12)$$

$$\text{or to } C^* / t' |Z/Z'| \cos(Ws - h - h^* - \pi)$$

if the magnet is the other way round

The proportionality is independent of u for small oscillations and W for all W (unless $L = L(W)$ or $C = C(W)$).

For a self consistent solution the total phase change around the system from $i(s)$ to $u(s)$ must be $2n(\pi)$, where $n = 0, 1, \dots$

That is,

$$h + h^* = n(\pi)$$

(the extra π is achieved by reversing the magnet if necessary)

$$\tan (n(\pi)) = \tan (h + h^*)$$

$$= \frac{WCR^* / (1 - W^2 LC) + WY / J [(W^*)^2 - W^2]}{1 - [WCR^* / (1 - W^2 LC)] [WY / J [(W^*)^2 - W^2]}}$$

$$= 0 \quad \dots (A.13)$$

This leads to

$$JCR^* [(W^*)^2 - W^2] + (1 - W^2 LC) = 0 \quad \dots (A.14)$$

$$W' = W^* [(1 + Y / (W^*)^2 JCR^*) / (1 + YL / JR^*)]^{1/2} \quad \dots (A.15)$$

ω' is therefore approximately equal to the natural frequency of the silicon oscillator provided that Y is small compared to R^* ; that is, the oscillator must have a much higher Q than the electric circuit.

Appendix B

Calculation of the drive power for one sensor

It has been noted that the amplitude of oscillation C^* should not exceed 1° to avoid hysteretic effects. However, we wish to have as large an amplitude as possible in order to maximise the signal modulation. Therefore suppose $C^* = 0.5^\circ$.

At resonance, C^* (Eqn. A.9) reduces to t'/WY where

$$Y = WJ/Q \quad \dots(B.1)$$

J being the mass moment of inertia and Q the quality factor. For one of our devices we measured W to be 4141 rad/s and Q to be 686. Thus, the torque t' required to produce this oscillation amplitude C^* is:

$$t' = W^2JC^*/Q = 9.1 \times 10^{-2} \text{ Nm} \quad \dots(B.2)$$

in which J was calculated from the natural frequency of the silicon oscillator using Eqn. A.11.

By placing the paddle in a known magnetic field produced by Helmholtz coils and noting the deflection using an optical lever, the magnetic moment $|m|$ of the SmCo magnet on the paddle was determined and found to be $5.3 \times 10^{-7} \text{ Am}^2$. Rearranging Eqn. 4 and setting v to 90° , we can calculate the magnetic field B required to produce torque t' :

$$B = t'/|m| = 17 \times 10^{-6} \text{ T}$$

From our measurements, we find that to create a 17 μT field between the pole pieces of the metallic glass, where the paddle is situated, a current of 0.17mA is required from the photodiode at this frequency. The conversion efficiency X of a typical silicon photodiode at 850 nm is 0.55 A/W and so we require $0.17 \times 10^{-3}/0.55 = 0.31 \text{ mW}$ of optical power to be reflected onto the photodiode. As the reflectivity of the silicon paddle at 850nm is 0.32 then approximately 1mW ($0.31/0.32$) of optical power is required to be incident on the oscillator in order to drive it at an amplitude of 0.5° .

Clearly, coating the paddle to improve its reflectivity (eg. with gold Fig. B.1) would reduce the power requirement considerably.

Appendix C.

Temperature dependence of the silicon oscillator

Ref. 43 has been used.

The natural angular frequency W^* of the silicon oscillator structure shown in Fig. 6 is given by:

$$(W^*)^2 = KG/Jl \quad \dots(C.1)$$

Taking natural logarithms and differentiating, the temperature coefficient can be written as:

$$(1/W^*)\partial W^*/\partial T = [(1/K)\partial K/\partial T + (1/G)\partial G/\partial T - (1/J)\partial J/\partial T - (1/l)\partial l/\partial T]/2 \quad \dots(C.2)$$

K is given by

$$K = nm^3[16/3 - 3.36m(1 - m^4/12n^4)n] \quad \dots(C.3)$$

Hence,

$$\begin{aligned} \partial K/\partial T = [16nm^2 - 13.44m^3 + 2.24m^7/n^4]\partial m/\partial T \\ + [16m^3/3 - 1.12m^8/n^5]\partial n/\partial T \quad \dots(C.4) \end{aligned}$$

Typically, $n = 100$ microns, $m = 4$ microns and

$$(1/n)\partial n/\partial T = (1/m)\partial m/\partial T = 2.4 \times 10^{-6} \text{ } ^\circ\text{C}^{-1}$$

Thus,

$$K = 3.3 \times 10^{-20} \text{ (metre)}^4$$

and $(1/K)\partial K/\partial T = 9.7 \times 10^{-6} \text{ } ^\circ\text{C}^{-1}$

$(1/l)\partial l/\partial T$ is the linear expansivity of silicon and so:

$$(1/l)\partial l/\partial T = (1/n)\partial n/\partial T = 2.4 \times 10^{-6} \text{ } ^\circ\text{C}^{-1}$$

The temperature dependence of the shear modulus is not known but as G is related directly to Youngs modulus we may expect the temperature dependence to be similar. Values for the temperature dependance of Youngs modulus vary from about -50 to -100 ppm/ $^\circ\text{C}$ and so we have estimated the temperature dependence of the shear modulus to be -80ppm/ $^\circ\text{C}$.

J, the mass moment of inertia of the paddle, is given by

$$J = m (a^2 + b^2)/12 \quad \dots(C.5)$$

where m is half the paddle mass (including the SmCo magnet) and a and b are defined in Fig. 6. Differentiating we obtain

$$\partial J/\partial T = m(2a\partial a/\partial T + 2b\partial b/\partial T)/12 \quad \dots(C.6)$$

since, $(1/a)\partial a/\partial T = (1/b)\partial b/\partial T = \text{linear expansivity,}$

$$\partial J/\partial T = 2J[(1/a)\partial a/\partial T] \quad \dots(C.7)$$

Therefore

$$(1/J)\partial J/\partial T = 2[(1/a)\partial a/\partial T] = 4.8 \times 10^{-6} \text{ } ^\circ\text{C}^{-1} \quad \dots(C.8)$$

The temperature dependence of the silicon is then

$$\begin{aligned} (1/W)\partial W/\partial T &= [(9.7-80-4.8-2.4) \times 10^{-6}]/2 \\ &= \text{approx. } -40 \text{ ppm}/^\circ\text{C} \end{aligned}$$

It is therefore clear that considerable effort will be required in temperature compensation if the 50ppm/ $^\circ\text{C}$ target is to be achieved for the whole transducer assembly. Alternatively a smaller operational temperature range or reduced accuracy must be specified.

Abbreviations, Acronyms and Symbols

A	Unrestrained bimetal cantilever deflection
A*	Effective area of bellows
A'	Illuminated area of paddle
B	Magnetic field
C	Capacitance in electrical circuit
C*	Oscillation amplitude of paddle
D	Force acting on a cantilever
E	Modulus of elasticity of bimetal
F	Force exerted on bellows due to external pressure, p or PLL figure of merit
F*	Residual force generated by a partially restrained bimetal cantilever.
F'	Force developed by a restrained bimetal cantilever
F''	Force required to be applied to a lever of length to produce a torque t.
FFT	Fast Fourier Transform
G	Shear modulus
I	Cantilever moment of inertia
I'	Incident light intensity on oscillator
IF	Intermediate frequency
J	Mass moment of inertia of paddle
J*	Polar moment of inertia
K	Torsional stiffness constant
L	Inductance in electrical circuit
LO	Local oscillator
M	Sensid number
N	Sensor number
P	Reflected optical power onto photodiode in sensor
PLL	Phase Lock Loop
Q	Quality factor of an oscillator

R	Reflectivity of paddle <u>or</u> fractional resolution (eg. 1 in 100)
R*	Resistance in electrical circuit
S	Tensile stress on paddle supports
SmCo	Samarium - Cobalt
SENSID	Sensor Interface Device
SYSTID	System Interface Device
T	Filter time constant <u>or</u> Temperature
T*	Temperature change or ranges
U	Magnetic flux
VCO	Voltage controlled oscillator
VLSI	Very large scale integration
W	Force applied to cantilever <u>or</u> base angular frequency <u>or</u> PLL natural frequency
W''	Full scale or maximum value of sensor angular frequency
W*	Natural angular frequency of silicon oscillator <u>or</u> PLL capture range
W'	Resonant angular frequency
X	Conversion efficiency of photodiode in Amps/Watt
Y	Mechanical damping coefficient
Z	Impedance
Z'	Inductor impedance
a	Paddle width <u>or</u> particle radius
a'	Specific thermal deflection of bimetal
b	Paddle thickness
b'	Bimetal strip width
c	Outer radius of torsion tube
d	Deflection (of cantilever free end, bellows etc).
f	Frequency
f*	Nominal centre frequency for ith oscillator
g	Length of lever attached to top of torsion tube

h	Phase angle
h*	Phase angle
i	Current produced by photodiode
i'	Inductor current
i*	Peak value of i
j	Square root of minus unity
k	Spring rate of bellows <u>or</u> PLL oscillator lock range
l	Length of paddle support <u>or</u> length of torsion tube
l'	Bimetal cantilever length
m	Mass of half paddle <u>or</u> Magnetic moment of Samarium Cobalt magnet <u>or</u> half thickness of paddle support
n	An integer (positive or zero) <u>or</u> half width of paddle support
p	External pressure on bellows
p/v	Private venture
q	Particle size scatter parameter
r	Inner radius of torsion tube
s	Bimetal thickness
t	Torque
t'	Peak value of torque produced by B acting on m.
u	Angle between incident beam and paddle normal in the paddle rest position
v	Angle between <u>m</u> and <u>B</u>
w	Wavelength of incident light
x	Distance between the point at which W is applied and the paddle
y	Angular twist of torsion tube
z	Half thickness of cantilever

Note

Where a symbol is defined as having more than one meaning, the meaning in use will be clear from the context.

DATE
FILMED
088